

Intracortical administration of pleiotrophin in ischemic stroke: investigating functional outcomes
and glial expression

by

Celestina Stefana Tanase

A thesis submitted in partial fulfillment of the requirements for the degree of
Master of Science

Neuroscience

University of Alberta

Abstract

Ischemic stroke is the leading cause of disability and third leading cause of death in Canada, exerting a serious burden on stroke survivors, their families, and healthcare resources. Characterized by brain damage due to loss of blood flow and oxygen supply, ischemic stroke is characterized by damage to brain tissue and chronic disability that most commonly affects sensation and movement of the upper limb. With rehabilitation, recovery from stroke is improved but is rarely complete. Current efforts focus on enhancing the extent of recovery following stroke to minimize the burden of disability on stroke survivors. This improvement in recovery could be achieved by improving the survival and regenerative capabilities of brain tissue following stroke. Pleiotrophin (PTN) is a protein that is abundantly expressed in utero and is associated with brain development by its diverse actions on different cell types existing in the brain. PTN has been documented to modulate the immune response, neuronal development, and myelination. In the present study, we sought to administer PTN to the cortical regions surrounding a stroke to investigate its effects on recovery from stroke-related functional deficits and brain responses to ischemic injury. Animals were administered an ischemic stroke affecting the forelimb and hindlimb sensorimotor cortex, followed by a delayed cortical injection of PTN. Functional deficits were assessed using two behavioural assays, the Tapered Beam task and String Pull task, which focused on measures of forelimb and hindlimb motor function. Brain tissue at varying timepoints post-stroke was investigated for PTN protein availability, markers of microglia (immune cells of the brain), astrocytes (multifunctional glial cells that form a protective scar following brain injury), and oligodendrocytes (brain cells necessary for myelination). Following stroke, only mild impairments in two sensorimotor tasks were detected. Performance in these behavioural assays was related to stroke size but unaffected by PTN treatment. Similarly, expression of the cell-

specific markers was related to timepoint following stroke, but not PTN treatment. The data presented in this study cannot clearly conclude the effects of PTN treatment on functional recovery and glial responses post-stroke. Tasks more sensitive to this stroke model and investigation of cell signaling related to PTN injection in tissue are needed in future studies investigating PTN as a therapeutic target in stroke recovery.

Preface

This thesis is an original work by Celestina Stefana Tanase. All animal research was conducted in accordance with the Canadian Council on Animal Care guidelines. All animal use protocols were approved by the University of Alberta Animal Care and Use Committee (AUP360).

Acknowledgements

Firstly, I would like to thank my supervisor Dr. Ian R. Winship for his constant support, guidance, and patience throughout my degree. You were a great motivator and incredibly dedicated to my work throughout the constant obstacles brought on by the pandemic. This thesis would not have been possible without the help of such a committed and resourceful supervisor.

I would also like to thank my committee members, Dr. Karim Fouad and Dr. Keith Fenrich, for their support and feedback during my time in this graduate program. As well, it was a pleasure to spend time in the Fouad Lab and explore spinal cord injury research as part of my NEURO 501 research project.

So much of the work compiled in this thesis would not have been possible without the help of numerous members of the Winship Lab and Neurochemical Research Unit. Thank you to Patricia Kent for consistently going above and beyond in helping me organize my experiments. Thank you to Mischa Bandet, John W. Paylor, and Eszter Szepesvari Wendlandt for being a wealth of knowledge and creative feedback throughout my time in the Winship Lab. As well, thank you to Faith Trinh, Jocelyn McConnell, and Amena Thraya for the time and commitment they provided to help bring every tiny detail of this project together. Every member of the Winship Lab has played a role in making my time while working on this thesis a lovely experience of learning and growth.

This work was only possible because of funding support provided by the Canadian Institutes of Health Research.

Finally, I would like to acknowledge the immense support provided by my family throughout this degree. My parents, Robert and Arina Tanase, have endlessly supported me throughout my many academic endeavours. They have had absolute faith and belief in my abilities

even when my own self-confidence wavered. Thank you for consistently setting an example of ambition and perseverance in the face of hardship.

Table of Contents

Abstract	ii
Preface	iv
Acknowledgements	v
List of Tables	ix
List of Figures	x
1. Introduction	1
<i>1.1 Ischemic Stroke Pathophysiology</i>	<i>1</i>
<i>1.2 Plasticity in Ischemic Stroke</i>	<i>3</i>
<i>1.3 Plasticity and Recovery</i>	<i>6</i>
<i>1.4 Post-Stroke Rehabilitation</i>	<i>7</i>
<i>1.5 Plasticity-Enhancing Treatments</i>	<i>10</i>
<i>1.6 Pleiotrophin</i>	<i>12</i>
2. Experimental Objectives	17
3. Hypothesis	18
4. Methods	19
<i>4.1 Animals</i>	<i>19</i>
<i>4.2 Experimental Groups</i>	<i>19</i>
<i>4.3 Behavioural Training and Testing</i>	<i>20</i>
<u>4.3.1 Tapered Beam Test</u>	<i>20</i>
<u>4.3.2 String Pull Test</u>	<i>21</i>
<i>4.4 Surgical Procedures</i>	<i>21</i>
<u>4.4.1 Photothrombotic Stroke</u>	<i>22</i>
<u>4.4.2 Cortical Microinjections</u>	<i>22</i>
<i>4.5 Tissue Processing and Immunohistochemistry</i>	<i>23</i>
<u>4.5.1 Transcardial Perfusion and Tissue Fixation</u>	<i>23</i>
<u>4.5.2 Tissue Freezing and Sectioning</u>	<i>23</i>
<u>4.5.3 Immunohistochemistry and Imaging</u>	<i>24</i>
<i>4.6 Statistical Analysis</i>	<i>24</i>
5. Results	26

5.1 Stereotaxic placement of photothrombotic strokes produced similar infarcts among treatment groups that were still visible 6 weeks post-stroke	26
5.2 Tapered Beam and String Pull tasks did not reveal deficits in injured groups regardless of treatment	26
5.3 Correlations in Tapered Beam and String Pull task measures to infarct surface area.....	28
5.4 Visualization of PTN at injection sites.....	29
5.5 Iba1 and GFAP fluorescence were pronounced following stroke, but unaffected by treatment	30
5.6 Myelination is not clearly altered by PTN.....	31
6. Discussion.....	33
6.1 Tapered Beam task and String Pull task measures detect minimal functional deficits due to photothrombosis targeted via stereotaxic coordinates	33
6.2 Cortical microinjection of PTN resulted in notable extracellular parenchymal expression of PTN in the ipsilesional cortex.....	35
6.3 Markers of glial reactivity were not significantly altered in the presence of exogenous PTN	36
6.4 Markers of OPCs were elevated after stroke, but myelination markers remained stable ..	39
7. Conclusion	40
Bibliography	43
Appendix I: Figures	72
Appendix II: Tables	90

List of Tables

- Table 1.** Information regarding animals that were used in the behavioural assay spanning 8 weeks, from training to endpoint
- Table 2.** Information regarding animals that were used for immunohistochemical analysis
- Table 3.** Training and testing schedule for animals during the behavioural study
- Table 4.** Immunohistochemistry (IHC) plan for antibodies and targets
- Table 5.** Descriptive statistics of total foot faults during Tapered Beam task
- Table 6.** Descriptive statistics of total foot faults normalized to baseline during Tapered Beam task
- Table 7.** Descriptive statistics of left foot faults during Tapered Beam task
- Table 8.** Descriptive statistics of left foot faults normalized to baseline during Tapered Beam task
- Table 9.** Descriptive statistics of total foot faults during Tapered Beam task for selected animals
- Table 10.** Descriptive statistics of total foot faults normalized to baseline during Tapered Beam task for selected animals
- Table 11.** Descriptive statistics of left foot faults during Tapered Beam task for selected animals
- Table 12.** Descriptive statistics of left foot faults normalized to baseline during Tapered Beam Task for selected animals

List of Figures

Figure 1. Diagram outlining pathways of interest on which PTN acts.

Figure 2. Coordinates of infarct area and injection sites.

Figure 3. Start and end points of tissue collection.

Figure 4. Surface area of visible infarct on formalin-perfused brains.

Figure 5. Behavioural outcomes following injury and treatment, assessed by the Tapered Beam and String Pull Tasks.

Figure 6. Tapered Beam performance when selecting for the largest observed strokes.

Figure 7. Correlation between stroke surface area and performance on Tapered Beam task measures.

Figure 8. Correlation between stroke surface area and performance on String Pull task measures.

Figure 9. Mean fluorescence intensity of PTN immunohistochemistry at 3 days and 14 days post-stroke.

Figure 10. Mean fluorescence intensity of Iba1 and GFAP to indicate reactivity of microglia and astrocytes, respectively, from 3 to 14 days post-stroke.

Figure 11. Iba1+ cells counted in the ipsilesional cortex normalized to Iba1+ cell count in the contralesional cortex at 7 days post-stroke.

Figure 12. Mean fluorescence intensity of MBP to indicate presence of myelin from 3 to 14 days post-stroke.

Figure 13. Mean fluorescence intensity of O4 to indicate presence of oligodendrocyte precursor cells from 3 to 14 days post-stroke.

1. Introduction

1.1 Ischemic Stroke Pathophysiology

Ischemic stroke results from a transient or permanent reduction of blood flow to either the entire brain, which is known as global ischemia, or a specific region of the brain, known as focal ischemia (Winship & Murphy, 2009). Without sufficient blood flow to the affected region, oxygen supply is greatly diminished, setting off a cascade of pathological events that contribute to cell death and loss of function (Carmichael, 2006; Winship & Murphy, 2009; Xing et al., 2012). Following this pronounced cell death, the affected region is no longer able to execute its usual functions. This contributes to the motor and sensory deficits that are commonly seen in stroke patients. In Canada, stroke is the leading cause of disability and the third leading cause of death (Government of Canada, 2017) . The burden of stroke on survivors, their families, and the healthcare system is also substantial, which has been evidenced by an increased number of annual visits to the family doctor to address the increased prevalence of multiple impairments and conditions (Obembe et al., 2019). Globally, the prevalence of stroke as a cause of both death and disability is rapidly increasing, with a 70% increase in incident strokes and 102% increase in prevalent strokes in from 1990 to 2019 (Feigin et al., 2022).

Ischemic stroke is a complex brain injury with a core region and penumbra. The core region is characterized by severe ischemia, which leads to anoxic depolarization and necrosis (Emsley et al., 2008). Early in the ischemic timeline, there is an area surrounding the lesion core known as the penumbra, which is made up of neurons that are functionally silent but are still viable, with an upregulation of both anti-apoptotic and pro-apoptotic proteins. (Demyanenko & Uzdensky, 2017; Emsley et al., 2008; Endres et al., 2008; Hossmann, 2006; Murphy & Corbett, 2009; Uzdensky,

2019). Over time, however, the core can expand because of the overproduction of reactive oxygen species, excitotoxicity, and cytoskeleton disruption processes that trigger neuronal death pathways, thus transforming viable penumbra tissue into infarct (Demyanenko & Uzdensky, 2017; Endres et al., 2008; Xing et al., 2012). In response to injury, glial cells surrounding the infarct become reactive to form the glial scar, primarily composed of rapidly proliferating astrocytes. The glial scar functions to contain the infarct core, but is also made up of growth-inhibitory molecules such as chondroitin sulphate proteoglycans (CSPG) that act as a barrier to axon sprouting and remyelination via their glycosaminoglycan (GAG) side chains (Fawcett & Asher, 1999; Silver & Miller, 2004; N. R. Sims & Yew, 2017).

Additionally, cerebral ischemia triggers a robust microglial and immune response. Enhanced activation of microglia has been observed to occur within minutes of ischemic injury in animal models, and can last for several weeks (Benakis et al., 2015; J. Huang et al., 2006; Ito et al., 2001; Tonchev, 2011; Xing et al., 2012; Xu et al., 2020). In the acute stages following stroke, microglial activation produces a strong inflammatory response that can be detrimental to central nervous system (CNS) tissue; however, chronically, microglia have been observed to produce protective molecules and play a phagocytic role in the damaged cortex (Benakis et al., 2015; Xu et al., 2020). A peripheral inflammatory response has also been observed following both transient ischemic attacks (TIA) and stroke, which is closely linked to activation of the hypothalamic-pituitary-adrenal axis (HPAA) and sympathetic nervous system (SNS) (Adiguzel et al., 2021; Emsley et al., 2008; Ross et al., 2007). Peripheral inflammation can contribute to an increased risk of developing systemic infection following stroke, which may worsen stroke outcome (Emsley et al., 2008). Further, modulating peripheral inflammation has been shown to affect lesion volume and inflammation in the cortex (Kolosowska et al., 2019).

The physiology of the ischemic brain is characterized by several processes that can promote recovery and provide neuroprotection, as well as degenerative processes including excitotoxicity, oxidative stress, and inflammation (Carmichael, 2003, 2006; Chamorro et al., 2016; Kerr et al., 2011; Rothman & Olney, 1986; Winship & Murphy, 2009). Together, these processes define the extent of injury and neuroplasticity present in the post-stroke brain, and thereby determine the extent of functional recovery.

1.2 Plasticity in Ischemic Stroke

In the ischemic cortex, there are both opportunities for and barriers to plasticity. Expression of growth-promoting genes in the perilesional area can promote axonal sprouting is significantly altered following ischemic stroke in rat models (Carmichael, 2003; Carmichael et al., 2005; Gorup et al., 2015; Stroemer et al., 1993, 1995). Trophic factors that promote neurite outgrowth and cell survival are elevated in the perilesional cortex after ischemic stroke, such as brain-derived neurotrophic factor (BDNF), nerve growth factor (NGF), and neurotrophin-3 (NT-3). (Barde, 1989; T.-H. Lee et al., 1998). Endogenous and enhanced expression of BDNF and NGF post-stroke are associated with reduction in infarct volume in stroke, neuroprotection, and the promotion of an anti-inflammatory response in other animal models of brain injury (Greenberg & Jin, 2006; Saito, 2004; S.-K. Sims et al., 2022; Uzdensky, 2018; Zou et al., 1999). In stroke survivors, high serum NGF is associated with good functional outcomes 3 months post-stroke and is higher in stroke patients than in control subjects (Luan et al., 2019). These trophic factors induce phosphorylation of downstream factors such as Growth-Associated Protein 43 (GAP43), which plays an important role in neurite formation and is elevated in the growth cones of growing neurites (Carmichael, 2003; Fournier et al., 1997; Geremia et al., 2010; Kobayashi et al., n.d.; Ng et al.,

1988; Stroemer et al., 1993, 1995). In mouse and rat models of ischemic stroke, GAP43 expression is elevated early after injury in the ipsilesional cortex, and this was also found to be true in post-mortem human brain tissue that after ischemic stroke (Gorup et al., 2015; Ng et al., 1988; Stroemer et al., 1993, 1995). GAP43 levels have also been observed to be elevated in both the cortex and spinal cord in a photothrombotic rat model (Sist et al., 2014). This upregulation of GAP43 was most pronounced at 14 days post-stroke and returned to control levels by 28 days post-stroke (Sist et al., 2014). Interestingly, GAP43 levels were correlated with upregulated expression of tumor necrosis factor- α (TNF- α) and interleukin-6 (IL-6), two pro-inflammatory markers that have been previously associated with plasticity (Hakkoum et al., 2007; Oshima et al., 2009; Parish et al., 2002; Saleh et al., 2011; Sist et al., 2014; Suzuki et al., 2009). The ischemic brain also generates plasticity-inhibiting molecules. The glial scar, though serving a protective function by containing necrotic tissue, contains CSPGs and other growth-inhibitory molecules that have been identified as barriers to plasticity and remyelination following ischemic stroke (Alia et al., 2017; Cua et al., 2013; Silver & Miller, 2004). The balance of plasticity-promoting and -inhibiting factors determines the extent of rewiring.

Neuroplasticity after stroke also includes the unmasking, or disinhibition, of previously latent neuron networks, which could be a result of homeostatic mechanisms including the downregulation of γ -aminobutyric acid (GABA) signalling (Jacobs & Donoghue, 1991; Kreisel et al., 2006; Wenner, 2011). Homeostatic plasticity refers to neurons aiming to function at a set level of electrical activity through negative feedback mediation (Murphy & Corbett, 2009; Takeuchi & Izumi, 2015; Wenner, 2011). Stroke induces injury to tissue, depriving connected regions of excitatory drive, and homeostatic mechanisms could reduce GABA signalling to compensate. Further, animal models of ischemic stroke have shown alterations in membrane properties of

neurons in the periinfarct regions that make them less excitable and demonstrated an impairment of synaptic transmission in the penumbra (Bolay et al., 2002; Gao et al., 1999). Stroke leads to diaschisis in regions functionally connected to the site of injury, typically manifested as a reduction in blood flow and metabolism (Bolay et al., 2002; Carmichael et al., 2004; Gao et al., 1999) in these regions. Physiological mechanisms could trigger structural neuroplasticity including axonal sprouting after ischemic injury, as synchronous activity of neurons has been observed in periinfarct tissue exhibiting axonal sprouting in an ischemic lesion, suggesting a link between neuronal electrical activity and post-stroke plasticity (Carmichael & Chesselet, 2002). In the photothrombotic mouse model, increased formation of dendritic spines in the perilesional cortex has been observed as early as 1 week post-injury, with new spines persisting for up to 6 weeks post-injury (Brown et al., 2007). Further, neurogenesis occurring after stroke in a mouse model has been shown to migrate towards the perilesional area, and is specifically associated with newly remodeled vasculature (Ohab et al., 2006).

Structural neuroplasticity and unmasking of latent networks occurring acutely after stroke could interact with rehabilitative interventions to contribute to cortical remapping (Kreisel et al., 2006). In the healthy mature brain, behavioural experience can modulate cortical functional representations. Transcranial magnetic stimulation (TMS) studies of humans have demonstrated that muscle representation in the motor cortex can be extremely diverse and differ depending on repeated use of specific motor skills, such as a larger hand representation among racket players (Kerr et al., 2011; Kleim, 2011). Likewise, after stroke surviving neurons can reorganize as a result of adaptive plasticity, supporting functional recovery (Winship & Murphy, 2009). Cortical remapping, the process by which sensory or motor signals are transferred to new cortical regions, typically an area neighbouring the infarct, occurs in animal models and humans following stroke

(Alia et al., 2017; Green, 2003; Levy et al., 2001; Murphy & Corbett, 2009; Overman & Carmichael, 2014). In rat models of stroke, new functional sensory representations replacing those disrupted by stroke have been observed in response to stimulation of affected limb or whisker (Dijkhuizen et al., 2001; Jablonka et al., 2010). Cortical reorganization after stroke has also been observed in humans undergoing physical therapy and constraint-induced movement therapy (CIMT) (Liepert et al., 1998, 2000). Ischemic stroke patients with good recovery of hand function often show increased cortical excitability in the contralesional hemisphere, showing that reorganization can occur ipsi- or contralesionally (Bütefisch, 2003).

1.3 Plasticity and Recovery

Growth-promoting environments in the ischemic brain may contribute to improved functional outcomes. Behavioural improvements occurring early after stroke, known as spontaneous recovery, are believed to be mediated by plasticity processes in the areas surrounding the infarct and the functional remapping of these surviving areas (Kerr et al., 2011; Nudo, 2007). Conversely, the adaptation of compensatory behaviours that avoid usage of the affected limb after injury has been shown to further reduce the representation of said affected limb in animal models (Allred et al., 2010; Nudo, 2007). Thus, the plasticity of cortex is associated with recovery and amplifying this plasticity or harnessing it with rehabilitative training may improve recovery. The use of enriched environments as a rehabilitative method in animal models has been shown to improve recovery and impact the extent of dendritic branching post-stroke (Biernaskie, 2004; Murphy & Corbett, 2009; Overman & Carmichael, 2014; Wieloch & Nikolich, 2006). CIMT or forced limb use (FLU), a rehabilitative therapy where the good limb is constrained during awake hours so that the patient is encouraged to use their paretic limb, has been shown to elicit greater

improvements in chronic deficits in humans (Liepert et al., 1998, 2000; Wolf et al., 2006) as well as animal models, where enhancements in cortical plasticity have also been observed with this therapy (Hosp & Luft, 2011; Hu et al., 2021; C. Zhao et al., 2020; S. Zhao et al., 2013). The use of CIMT in humans as a rehabilitative intervention improves functional outcome and is accompanied by neural plasticity, which has been evidenced by TMS and functional magnetic resonance imaging (fMRI) data (Liepert et al., 1998, 2000; Szaflarski et al., 2006). The process of cortical remapping as a result of activity and behavioural intervention occurs within the critical period of elevated plasticity following ischemic stroke (Murphy & Corbett, 2009). Modulating this critical period using pharmacological interventions, such as reducing GABA_A-mediated inhibition and inducing the expression of the growth-promoting molecule brain derived neurotrophic factor (BDNF), has also been demonstrated to improve functional recovery and contribute to remapping of motor areas in a mouse model of ischemic stroke (Alia et al., 2016; Clarkson et al., 2011). Enhancing plasticity may therefore promote functional recovery and cortical remapping, and is an attractive therapeutic target.

1.4 Post-Stroke Rehabilitation

Many stroke survivors must cope with functional disabilities, such as weakness or paresis of the extremities contralateral to the infarct (Carmichael, 2003, 2006; Nakayama et al., 1994). In clinical settings, acute interventions for ischemic stroke focus on reperfusion to rescue penumbral tissue. Recombinant tissue plasminogen activator (rtPA) is a pharmacological intervention that functions to break down clots that are obstructing blood flow to the brain and reperfuse ischemic tissue (Hacke, 1995). More effective recanalization can now be achieved with mechanical thrombectomy, which involves the physical removal of a blood clot in a brain artery via customized

catheters (W. S. Smith et al., 2008). However, recovery is incomplete for most survivors even with successful recanalization. The majority of recovery of upper extremity function, one of the primary disabilities of stroke, has been observed to happen within the first 3 months following stroke, after which disability persists (Wade et al., 1983). Assessment of upper extremity paresis in the Copenhagen Stroke Study found that the best possible outcome for upper extremity function was achieved at 9 weeks post-stroke at the latest, and 3 weeks-post stroke at the earliest (Nakayama et al., 1994). The importance of early rehabilitative intervention has been emphasized in an animal model of stroke, where the delayed introduction of an enriched rehabilitative environment resulted in poorer recovery of limb function 5 weeks following middle cerebral artery occlusion (Biernaskie, 2004). Training too early, however, can exacerbate neural injury, even in the presence of functional recovery (Farrell et al., 2001; Kozlowski et al., 1996; Risedal et al., 1999). Immobilizing the good limb to promote usage of the affected limb immediately after stroke resulted in larger infarct and less dendritic branching (Kozlowski et al., 1996). Meanwhile, in a gerbil model of brain ischemia, placing the animals in enriched environments for rehabilitation 3 days post-injury improved performance on Open Field and T-Maze tests, measuring willingness to explore and spatial learning, respectively (Farrell et al., 2001). However, these animals also showed a reduction in CA1 cells, indicating more cell death (Farrell et al., 2001). Delaying environmental enrichment as much as 5 days post-stroke in rats, however, still resulted in functional improvement in spatial learning while also promoting neurogenesis in the affected hippocampus (Tang et al., 2019). In A Very Early Rehabilitation Trial (AVERT) in humans, mobilizing as early as 24 hours post-stroke and introducing a higher dose of physical therapy was associated with reduced likelihood of favourable outcome at 3 months post-stroke, but did not affect quality of life when assessed 12 months post-stroke (Bernhardt et al., 2006; Langhorne et

al., 2010, 2017). However, introducing rehabilitation at 72 hours post-stroke in patients that have been treated with rtPA was associated with a higher likelihood of functional independence at time of discharge when compared to patients that had been treated with rtPA but did not receive early rehabilitation (Momosaki et al., 2016). This evidence highlights an early and relatively small window for optimal functional recovery following ischemic stroke, while also cautioning against intervening too early.

Functional disabilities after stroke can continue to persist despite rehabilitative interventions. First-time cortical ischemic stroke survivors that were assessed 4 years post-stroke as having achieved adequate motor function in the affected arm still reported avoidance of using the affected arm and complaints of poor arm function (G. Broeks, et al., 1999). Further, it is estimated that over half of ischemic strokes display combined sensorimotor deficits (Kessner et al., 2016). Somatosensory input plays an important role in motor control. A study of 207 stroke patients found that extremity paresis and disability was more common in patients with somatosensory deficits than those with intact sensory inputs (Andersen et al., 1995). This evidence suggests that impaired somatosensation can negatively impact motor recovery following stroke, and that sensorimotor deficits, while common, may face a more complicated path to recovery. While the window of optimal rehabilitation can be difficult to pinpoint, the timecourse of enhanced plasticity of surviving brain tissue likely defines these windows for recovery.

The time course of stroke recovery in both humans and animal models is important to consider when developing interventions and studying possible therapeutic targets. In animal models, most functional recovery from stroke takes place within the first month following injury with significant remodelling of dendritic arbours happening in the first 2 weeks, but changes in dendritic branching and cortical maps can be observed to continue up to 8 weeks post-stroke

(Brown et al., 2007, 2009; Krakauer et al., 2012). Comparatively, in humans, most functional recovery from stroke occurs by 3 months following the injury (Krakauer et al., 2012; Wade et al., 1983). Furthermore, investigation of changes in Fugl-Meyer Assessment (FMA) scores, the standardized test for assessing sensorimotor recovery after stroke, in humans and animals helped define the proportional recovery rule (PRR) (Kundert et al., 2019). The PRR states that, with the provision of rehabilitative therapy, the extent of functional recovery occurring within the 3 to 6 months following stroke is approximately 70% of the maximum achievable improvement on the FMA (Kundert et al., 2019). The PRR serves as a benchmark for assessing whether a new intervention enhances function beyond expected spontaneous recovery (Hawe et al., 2019). Therefore, with greater initial impairment, there is also a greater potential for improvement. It is important to note that there is a subset of individuals who do not meet this expected recovery, known as nonfitters (Hawe et al., 2019). A proposed neuroanatomical explanation for this is that nonfitters have been shown to have poor corticospinal tract (CST) integrity (Byblow et al., 2015; M.-C. Smith et al., 2017). Therefore, the presence of nonfitters may be greater in disability requiring a functional CST for recovery, such as upper limb impairment (M.-C. Smith et al., 2017). The importance of spinal plasticity in recovering function after ischemic stroke has also been observed in animal models, where expression timelines of growth-promoting molecules in the spinal cord occur during periods of recovery and define thereafter (Sist et al., 2014).

1.5 Plasticity-Enhancing Treatments

Enhancing plasticity after stroke may facilitate a greater degree of functional recovery. Noninvasive brain stimulation (NIBS) functions by using tools such as TMS and transcranial direct current stimulation (tDCS) to facilitate cortical reorganization (Hara, 2015). Tools like TMS and

tDCS can upregulate excitability in the injured cortex, which has been associated with improved performance on functional motor tasks (F. C. Hummel & Cohen, 2006; F. Hummel & Cohen, 2005; Kleim, 2011; Pomeroy et al., 2007; Sandrini & Cohen, 2013). Manipulating behaviour through physical and occupational therapy also promotes functional recovery and helps patients with chronic deficits to adapt after stroke (Kerr et al., 2011). As noted, CIMT has been shown to elicit greater improvements in chronic deficits in humans (Liepert et al., 1998, 2000; Wolf et al., 2006) as well as animal models, where enhancements in cortical plasticity have also been observed with this therapy (Hosp & Luft, 2011; Hu et al., 2021; C. Zhao et al., 2020; S. Zhao et al., 2013).

While rehabilitative therapies can be effective in achieving functional recovery, maximal benefits are only obtained during the short critical period for plasticity that follows stroke. Many preclinical interventions therefore focus on reducing barriers to plasticity or enhancing plasticity in the injured cortex in order to maximize the period of time in which patients can benefit from rehabilitative therapies. CSPGs are significantly increased after stroke and known barriers to plasticity (Carmichael et al., 2005; Cua et al., 2013; L. Huang et al., 2014; S. Li & Carmichael, 2006; Silver & Miller, 2004; Yiu & He, 2006). The use of chondroitinase ABC (ChABC), an enzyme that breaks down CSPGs, has been pursued as a therapeutic intervention in neural injury (Barritt et al., 2006; Bradbury et al., 2002; Carter et al., 2011; X. Chen et al., 2014; García-Álías et al., 2009; H. Lee et al., 2010; Soleman et al., 2012). Intra-infarct perfusions of ChABC in a rat model of ischemic stroke rescued perilesional neurons and promoted the expression of GAP43 and synaptophysin, which is involved in synaptogenesis (X. Chen et al., 2014). CSPGs and the glial scar, however, also play a protective role, and their degradation could harm surviving tissue (Gleichman & Carmichael, 2014; Silver & Miller, 2004; N. R. Sims & Yew, 2017). Other studies have therefore attempted to enhance spinal plasticity to improve functional recovery after stroke.

Spinal delivery of ChABC to break down CSPGs and therefore reduce inhibition of spinal plasticity has been shown to improve functional recovery and promote sprouting of CST fibres after ischemic stroke affecting forelimb sensorimotor function (Soleman et al., 2012; Wiersma et al., 2017). Notably, this promotion of plasticity was also seen when spinal injections of ChABC were administered in chronic stroke, after the window for spinal plasticity has closed (Wiersma et al., 2017), suggesting it is possible to reopen a window for recovery. The effects of ChABC on functional recovery are promising and support investigating other proteins that interact with CSPGs as possible therapeutic targets.

1.6 Pleiotrophin

Pleiotrophin (PTN), or heparin-binding growth-associated molecule (BB-GAM), is an 18-25 kDa protein that is present in high levels in the developing brain and declines in the progression to adulthood (González-Castillo et al., 2015; Kadomatsu & Muramatsu, 2004). During development, PTN plays important roles in cell proliferation and neurite outgrowth. In the rat nervous system, PTN mRNA has been detected as early as embryogenesis day 9 (E9) in multipotent precursor cells that go on to form neurons and glia, with levels peaking between postnatal days 7 (P7) and P14 (Wanaka et al., 1993). A similar pattern of expression was found in the rat spinal cord (Wanaka et al., 1993). Furthermore, in the neonatal rat brain, PTN expression was found to be closely associated with developing fibre tracts (Rauvala et al., 1994). In the mouse cerebellum, high levels of PTN mRNA were detected at P0 which then went on to decline towards adulthood, while PTN protein levels detected by Western blot analysis were high within the first 2 postnatal weeks and then rapidly declined between P21 and adulthood (Basille-Dugay et al., 2013). Cultured embryonic mouse neurons treated with recombinant PTN upregulated GAP43

expression via activation of the anaplastic lymphoma kinase (ALK)/glycogen synthase kinase 3 β (GSK3- β)/ β -catenin pathway (Yanagisawa et al., 2010) (see Figure 1). In zebrafish embryos, cell transfection with a PTN expression plasmid enhanced neurite outgrowth (Chang et al., 2004). Evidence from rat hippocampal culture has also shown that PTN synthesized by glia enhances neurite outgrowth, while in the embryonic pig brain PTN binds heparin sulfate (HS) chains of syndecan-3 and chondroitin sulfate (CS) chains of phosphacan to mediate neurite extensions and neuronal migration (Bao et al., 2005). PTN and two of its known receptors, ALK and receptor protein tyrosine phosphatase ζ (RPTP- ζ), are found in the hippocampus, where they are believed to modulate plasticity during learning (González-Castillo et al., 2015). This evidence suggests that PTN plays an important role in processes that are observed in the critical period of plasticity for the developing brain.

While its expression is reduced in adulthood, PTN levels have been observed to fluctuate in certain contexts. Elevated levels of PTN have been observed in cancer, a disease of uncontrolled cell proliferation, and PTN levels are positively correlated with histopathological grade of astrocytomas (Kadomatsu & Muramatsu, 2004; Peria et al., 2007). A model of peripheral sciatic nerve injury in mice also demonstrated high levels of PTN in the injured nerve, exhibiting a pattern of expression that first favoured neurons and new Schwann cells early after injury, then macrophages 2 weeks post-injury (Blondet et al., 2005). PTN expression has also been observed in CNS disease and injury. In a rat model of Parkinson's Disease (PD), upregulation of PTN mRNA and protein was seen in the striatum up to 3 weeks following lesion induction (Hida et al., 2003). A model of targeted pericyte loss in mice that produced circulatory failure, as defined by cerebral blood flow (CBF), also reported a reduction in PTN mRNA in cortex and protein in cerebrospinal fluid (CSF) (Nikolakopoulou et al., 2019). Rapid pericyte loss is observed in several

CNS disorders, including the early stages of ischemic stroke (Nikolakopoulou et al., 2019). Finally, PTN has also shown a unique pattern of expression following ischemic stroke. In rats that underwent middle cerebral artery occlusion (MCAO), PTN mRNA and protein was elevated in reactive astrocytes in the perilesional area (Yeh et al., 1998). At day 3 post-stroke, PTN mRNA and protein expression was seen in macrophages near vessels within the infarct, and at day 7 this expression was also seen in hyperplastic blood vessels and their endothelial cells (Yeh et al., 1998). By 14 days post-stroke, PTN immunoreactivity was diminished (Yeh et al., 1998). This evidence displays a potential role for PTN in disorders of the CNS.

As a protein that has been identified to enhance plasticity, modulation of PTN has been studied as a means for improving disease outcomes. Oligodendrocytes are essential for myelination throughout the CNS, and focal ischemic injury in humans can cause extensive damage to myelinated regions known as white matter (Dewar et al., 2003; Wang et al., 2016). Culturing fetal human oligodendrocyte precursor cells (OPC) with PTN increased the cytosolic accumulation of beta-catenin and maintained proliferative expansion of OPCs (McClain et al., 2012). Importantly, it was also shown that inhibition of GSK3- β , which is downstream of PTN through the receptor ALK, and a lentiviral knock-down of RPTP- β/ζ , which is negatively regulated by PTN, had similar effects on beta-catenin increased T cell factor (TCF)-dependent transcription, a process that is related to the suppressed differentiation of OPCs (McClain et al., 2012) (see Figure 1). PTN can also have profound effects on microglia and astrocytes. In rat microglial culture that is subjected to the oxygen glucose deprivation (OGD) model, treatment with PTN promotes microglial proliferation and the secretion of BDNF and ciliary neurotrophic factor (CNTF) at 8 hours post-reperfusion (Miao et al., 2012). In transgenic mice overexpressing PTN protein, lipopolysaccharide (LPS)-mediated astrocytosis was attenuated, while cytokine expression was

upregulated and microglia in this model of neuroinflammation show enhanced hypertrophism (Fernández-Calle et al., 2017). There is a positive correlation between mRNA of pro-inflammatory markers TNF- α and inducible nitric oxide synthase (iNos) with PTN mRNA in the prefrontal cortex (PFC) of transgenic mice overexpressing PTN that have been treated with LPS, suggesting that PTN may be a mediator of neuroinflammation (Fernández-Calle et al., 2020). Furthermore, pharmacological inhibition of the PTN receptor RPTP- β/ζ in LPS-treated mice enhances microglial proliferation, suggesting that PTN may be exerting its mediating effects on neuroinflammation through its negative regulation of RPTP- β/ζ (Fernández-Calle et al., 2020). Exogenous PTN also has promising effects on neural plasticity processes. Treating dopaminergic cell cultures with PTN increased their proliferation and promoted survival (Hida et al., 2003). Hippocampal cell cultures overexpressing the full-length isoform of RPTP- β/ζ showed a decrease in dendritic synapses; however, treatment with PTN reversed this effect (Asai et al., 2009). PTN treatment of neuronal culture has also been shown to reverse the growth-inhibitory effects of CSPGs by binding CS side chains and inhibiting binding of protein tyrosine phosphatase σ (PTP- σ) to CSPGs (Paveliev et al., 2016). Furthermore, cortical PTN injections in a brain prick injury resulted in a denser dendritic tuft and a greater number of apical dendrites (Paveliev et al., 2016). In a spinal cord injury (SCI) model, PTN injection resulted in an increased number of axons traversing the injury site at 14, 21, and 28 days post-injury (Paveliev et al., 2016). This evidence suggests that PTN can improve the plasticity of cortical and spinal projections in injury contexts, as well as reverse the negative effects of CSPGs without digesting them.

PTN is thus a promising target for negating the degenerative effects of the ischemic cascade and potentially enhancing the window for plasticity to improve functional outcome in ischemic stroke. PTN has been shown to contribute to OPC proliferation, which can aid in the myelination

of new neurons and repairing white matter damage. Amplifying microglial responses in neuroinflammation has the potential to improve the phagocytic response of microglia following stroke. PTN's close association with microvasculature following ischemic stroke could promote the survival of new neurons, as the post-stroke processes of angiogenesis and neurogenesis are closely related (Ohab et al., 2006). Furthermore, PTN can regulate plasticity by reversing the growth-inhibitory effects of CSPGs, which are abundant in the glial scar, as well as by activating ALK to promote downstream upregulation of GAP43 and inhibiting RPTP- β/ζ to improve dendritic branching.

2. Experimental Objectives

The objective of this research is to elucidate the effects of exogenous PTN adjacent to the infarcted tissue in a photothrombotic stroke in mice. We measured functional recovery from a photothrombotic lesion of the right sensorimotor forelimb and hindlimb cortex, as assessed by the Tapered Beam Test, which indicates limb function while walking and bilateral motor function, and the String Pull Test, which indicates postural function and forelimb function while performing a pulling motion. Additionally, we examined tissue-level indices of PTN action including activation of astrocytes and microglia, as indicated by glial fibrillary acidic protein (GFAP) and ionized calcium-binding adapter molecule 1 (Iba1); and myelination and proliferation of oligodendrocyte precursor cells, as indicated by expression of myelin basic protein (MBP) and O-antigen (O4).

3. Hypothesis

We hypothesized that if animals administered intracortical injections of PTN will exhibit greater functional recovery in the String Pull and Tapered Beam tests when compared to vehicle controls. We also predicted increased of Iba1 and GFAP and increased expression of O4 and MBP near PTN injection sites in the cortex.

4. Methods

4.1 Animals

All experimental procedures were performed on male and female C57BL/6J mice, age 24 to 32 weeks old. Animals were housed in groups of three to five per cage under standard laboratory conditions of 12:12 hour light:dark cycles with temperature controlled at 22°C. Mice were fed a diet of standard laboratory chow *ad libitum*. Water was available *ad libitum*. Animals were allowed to acclimatize to the facility for 1 week before commencing any experimental procedures. All animal use was approved by The University of Alberta Animal Care and Use Committee and all animal protocols were conducted in accordance with Canadian Council on Animal Care Guidelines.

4.2 Experimental Groups

Our aim was to assess whether cortical delivery of PTN during the subacute phase following a photothrombotic stroke (2 days post-injury) could enhance adaptive plasticity and improve outcomes on tests of functional recovery. We investigated motor and sensory function of the forelimbs and hindlimbs, as well as anatomical and physiological changes in the affected and spared cortices. Mice were divided into six groups: stroke and sham groups with cortical injections of vehicle solution (phosphate buffered saline, PBS), stroke and sham groups with cortical injections of low-concentration PTN (250 ug/ml), and stroke and sham groups with cortical injections of high-concentration PTN (5 mg/ml). These animals were assessed on behavioural tasks for 6 weeks post-stroke. In a separate cohort, brains from animals receiving PBS and high-concentration PTN were also extracted at the following timepoints after stroke: 3 days, 7 days, 14

days, and 28 days. These animals did not undergo behavioural testing. A total of 60 animals will be used for the behavioural study and 48 animals for the acute study. See Tables 1 and 2 for details on experimental group numbers used in this thesis.

4.3 Behavioural Training and Testing

For both behavioural tasks, animals were trained in a 2-week period alternating 5 days of training and 2 days of rest. Animals were rewarded after each training session with sucrose pellets. Stroke induction surgery immediately followed day 14 of the training schedule. After stroke induction, animals were assessed at every week post-injury for 6 weeks. Naive animals instead had a 7-day rest period following day 14 of their training schedule. See Table 3 for detailed training and assessment schedule.

4.3.1 Tapered Beam Test

The Tapered Beam Test was carried out as previously described (Ardesch et al., 2017). An automated touch sensor installed on a 100 cm beam that becomes progressively narrower (from 3.5 cm to 0.5 cm) sensed foot faults as the mouse crossed. During the two-week training period, animals walked across the beam for 5 days each week and 5 trials each day. During post-stroke assessment, 3 trials were performed for each animal and the mean of these trials was used to indicate their performance at the given timepoint. Animals were rewarded with sugar pellets throughout training and testing. Analysis of foot faults was automated using capacitive touch sensors connected to a Raspberry Pi single-board computer to process and store data using a custom Python software. The outcome measures investigated here are total foot faults and left foot

faults. This behavioural test has been validated in the photothrombotic stroke model in mice up to 6 days post-stroke (Ardesch et al., 2017).

4.3.2 String Pull Test

The String Pull Test was carried out as previously described (Blackwell, Banovetz, et al., 2018). During the first week of training, mice were trained in home cages where they were allotted 1 hour to pull different lengths of string, half of which contained a sugar pellet reward. During the second week of training, the same style of training was performed in the testing apparatus, a clear box with slits at the top allowing for strings to be hung. Finally, for baseline measures pre-stroke and post-stroke assessment, 3 trials were filmed, each followed by a sugar pellet reward. Videos of mice pulling string were trimmed down to the first four consecutive pulls of each string, and the videos were renamed to blind individual conducting analysis. Analysis of these videos was performed using a MATLAB analysis package, which characterizes the whole-body motion throughout a given videoclip (Inayat et al., 2020). With this analysis, we investigated bimanual coordination, body angle, and left-hand reach throughout the string-pulling motion. This behavioural test has been validated for use in uninjured C57BL/6J and Swiss Webster Albino mice (Blackwell, Banovetz, et al., 2018; Inayat et al., 2020) and in rats with unilateral ischemic injury to the forelimb sensorimotor cortex (Blackwell, Widick, et al., 2018).

4.4 Surgical Procedures

Surgical procedures were performed in animals deeply anesthetized with 1.5-2% isoflurane (in 30% nitrogen and 70% oxygen) at a flow rate of 1 L/min. Body temperature was maintained at 37°C with a rectal temperature probe and heating pad. All animals had incisions sutured and were

administered bupivacaine subcutaneously (0.003 mg/g body mass) as post-operative analgesic, then recovered in a cage with a heating pad maintained at 37°C. See Figure 1 for coordinates of photothrombotic stroke and cortical microinjections.

4.4.1 Photothrombotic Stroke

Mice were mounted in a stereotaxic frame and the right forelimb and hindlimb sensorimotor cortex was located using stereotaxic coordinates (0.75 to 2.75 mm medial/lateral [M/L], -1.75 to +1.75 mm anterior/posterior [A/P]; see Figure 2). This region was chosen according to mouse motor cortex maps defined by intracortical microstimulation (ICMS) studies (C.-X. Li & Waters, 1991; Tennant et al., 2011). A thin window was drilled over the 2 mm x 3.5 mm area, followed by an intraperitoneal injection of 100 mg/kg Rose Bengal in saline. The area around the thinned region was blacked out and, 10 minutes after intraperitoneal injection, the thinned skull was illuminated with a collimated beam of green laser light (532 nm, 17 mW; ~4.0 mm in diameter) for 20 minutes to activate the Rose Bengal and occlude all illuminated cortical vasculature, creating a focal ischemic lesion. Animals in sham groups were treated the same, with the exclusion of illumination of the thinned skull. This model was chosen for its ability to target defined areas of the cortex and high reproducibility (H. Li et al., 2014).

4.4.2 Cortical Microinjections

Mice were mounted in a stereotaxic frame and the target injection regions were located using stereotaxic coordinates (3 mm M/L and 0 mm A/P, 1.75 mm M/L and -2 mm A/P, and 1.75 mm M/L and 2 mm A/P; see Figure 2). Each region was drilled until the skull was thin enough to puncture, avoiding injury to blood vessels and brain tissue. At each region, 0.5 uL of either high

dose PTN (5 mg/ml in phosphate buffered saline [PBS]), low dose PTN (0.25 mg/ml in PBS), or vehicle (PBS) was injected at a depth of 0.75 mm using a Hamilton syringe. Injection sites were covered with bone wax.

4.5 Tissue Processing and Immunohistochemistry

4.5.1 Transcardial Perfusion and Tissue Fixation

Animals were administered 20% urethane intraperitoneally at a dose 0.015 ml/g body mass to induce endpoint anesthesia. When pedal reflexes were absent, the thoracic cavity was cut open to expose the heart while animal was pinned to 85-degree tray. A blunted needle tip connected to a perfusion pump was inserted into the left ventricle. A small incision was made in the right atria, and then approximately 5 mL of 0.9% saline solution was flushed through the animal, followed by approximately 15 mL of 1:10 formalin solution. Brain was extracted from perfused animal and stored in 1:10 formalin for 24 hours at 4°C, followed by 30% sucrose for 3 days at 4°C.

4.5.2 Tissue Freezing and Sectioning

Prior to freezing, brains were photographed with a dorsal view and these images were used for calculating infarct surface area using ImageJ software. Brain tissue was frozen in Optimal Cutting Temperature (OCT) Compound in isopentane over dry ice so that it was attached to a filter paper by the caudal end. Following freezing, tissue was stored at -20°C. A Leica Cryostat was used to section the tissue to collect coronal slices of brain tissue at a thickness of 30 microns over 8 series. See Figure 3 for anatomical guide of where tissue collection begins and ends.

4.5.3 Immunohistochemistry and Imaging

See Table 4 for detailed dilutions and immunohistochemistry (IHC) antibodies. Brain tissue slides were washed in PBS 3 times for 10 minutes each, after which they were incubated with a blocking solution of 10% Universal Blocker (UB) and 90% PBS 0.1% Triton X-100 (0.1% Triton X-100 in PBS, PBS_{Tx}) for 1 hour at room temperature. Slides were then incubated overnight with the primary antibody solution, prepared with the appropriate antibody dilutions in 2% UB, 2% Bovine Serum Albumin (BSA), and 96% PBS_{Tx}. Slides were washed in PBS 0.1% TWEEN 20 (0.1% TWEEN 20 in PBS, PBS_{tween}) twice and in PBS once for 10 minutes each wash, then incubated for 1 hour with the secondary antibody solution, prepared with the appropriate antibody dilutions in 2% UB, 2% Bovine Serum Albumin (BSA), and 96% PBS_{Tx}. After this incubation period, slides were washed in PBS 0.1% TWEEN 20 (0.1% TWEEN 20 in PBS, PBS_{tween}) twice and in PBS once for 10 minutes each wash, then mounted with DAPI or FluoroMount and coverslipped. Following immunohistochemistry, slides were stored at 4°C. Slides were imaged using an epifluorescent microscope.

4.6 Statistical Analysis

Statistical analysis was performed using GraphPad Prism v9. For Tapered Beam Test, the number of total and left foot faults was obtained from the touch sensors and averaged over three trials per timepoint for each animal. For String Pull Test, the automated MatLab software was used to obtain measures of bimanual coordination (correlation between the vertical distance each hand travels during motion), left hand Y-reach (vertical distance travelled by the left hand during reaching motion), and posture (the angle of body during string pulling and the height of body during string pulling). For epifluorescent images collected of immunohistochemistry slides,

ImageJ was used to perform intensity measurements and cell counts to quantify histological changes at each timepoint and in each treatment group. Outliers were identified using the ROUT method. The Shapiro-Wilk test was used to determine if data sets adhered to normal distribution. If normal distribution could be assumed, two-way analysis of variance (ANOVA) was used to determine main effect of treatment and time in behavioural data and one-way ANOVA was used to determine main effect in histological data. If normal distribution could not be assumed, the Kruskal-Wallis test was used to determine main effect. Researcher was blinded during the analysis of collected behavioural data and images.

5. Results

5.1 Stereotaxic placement of photothrombotic strokes produced similar infarcts among treatment groups that were still visible 6 weeks post-stroke

While infarct volume in a rapidly developing photothrombotic stroke would not be affected by delayed PTN administration (and thus infarct volume was not measured), verification of stroke location was performed. Formalin-perfused brains were photographed with a millimetre scale, then these images were used to verify and measure surface area of visible infarct with the polygon tool in ImageJ/FIJI. The infarct was identifiable by an area of scarring surrounded by indented or “caved-in” brain tissue. Figure 4 shows the mean surface area of the infarcts in each treatment group, with individual values graphed and the error bars displaying standard deviation. No main effect of treatment on stroke surface area was observed ($P=0.631$), suggesting negligible variation in stroke size between treatment groups.

5.2 Tapered Beam and String Pull tasks did not reveal deficits in injured groups regardless of treatment

The experimental timeline for stroke induction and behavioural assays is displayed in Figure 5A. Baseline measurements were taken twice before stroke induction, then post-stroke measures were taken every week following stroke for both Tapered Beam and String Pull tasks. All control groups (Naive, PBS-Sham, Low PTN-Sham, and High PTN-Sham) were pooled to form a “Controls” group for comparing against injured animals of different treatments. In Figure 5B, mean total foot faults of each experimental group per timepoint are shown. Two-way ANOVA revealed a main effect of time ($P=0.015$); however, Šídák’s multiple comparisons test revealed no

significance between timepoints for any of the treatment groups. The mean and standard deviation of total foot faults for each group at each timepoint can be found in Table 5. In Figure 5C, the mean total foot faults have been normalized to baseline measurements. The baseline measurement used for normalizing was the mean total foot faults of the two baseline timepoints. Two-way ANOVA revealed no main effects for normalized total foot faults. The mean and standard deviation of total foot faults normalized to baseline of each group at each timepoint can be found in Table 6. Figure 5D shows the mean foot faults performed with the left feet, which is the stroke-affected side. Though two-way ANOVA revealed a main effect of time ($P < 0.001$), Šídák's multiple comparisons test revealed no significant comparison between timepoints within any of the treatment groups. The mean and standard deviation of left foot faults for each group at each timepoint can be found in Table 7. In Figure 5E, the mean left foot faults for each group have been normalized to baseline using the same method as that used for normalization of total foot faults. 3 animals in the PBS-Stroke group had a baseline measurement of left foot faults of 0, so they were excluded from this measure. Two-way ANOVA revealed a main effect of time ($P = 0.041$) and Šídák's multiple comparisons test revealed a significant difference between mean left foot faults at 4 weeks and 6 weeks post-stroke in High PTN/Stroke animals. No other significant comparisons were observed. The mean and standard deviation of left foot faults normalized to baseline for each group at each timepoint can be found in Table 8.

Figures 5F-H display performance on the String Pull task for select animals. Five randomly selected animals from the Naive, High PTN-Stroke, and PBS-Stroke groups were analyzed on String Pull task measures at the 1 week post-stroke timepoint. Figure 5F shows mean body angle during string pulling motion at 1 week post-stroke. The Kruskal-Wallis test revealed no main effect ($P = 0.145$). Figure 5G shows mean bimanual coordination, a measure of how well subjects alternate

their hand motions during string pulling, at 1 week post-stroke. Ordinary one-way ANOVA revealed no main effect ($P=0.056$). Figure 5H shows the mean Y-Reach of the left hand, or the vertical distance travelled by the left hand during the reaching motion of string pulling, at 1 week post-stroke. Ordinary one-way ANOVA revealed no main effect ($P=0.935$).

5.3 Correlations in Tapered Beam and String Pull task measures to infarct surface area

Due to the lack of clear stroke-related deficits in these tasks, performance was probed further and correlated with surface area measurement of stroke size. The animals with the largest infarct surface areas were first selected for further investigation into behavioural performance, regardless of treatment group. The mean stroke surface area of these 8 animals was 2.09 mm^2 with a standard deviation of 0.960 mm^2 .

Figure 6A shows mean total foot faults at each timepoint for naive animals and the selected stroke animals. Two-way ANOVA revealed no main effects. The mean and standard deviation of total foot faults for each group at each timepoint can be found in Table 9. In Figure 6B, mean total foot faults were normalized to baseline and two-way ANOVA revealed a main effect of time ($P=0.034$), but Šídák's multiple comparisons test showed no significant differences timepoints within any treatment group. The mean and standard deviation of total foot faults normalized to baseline for each group at each timepoint can be found in Table 10. In Figure 6C, mean left foot faults made at each timepoint are shown. Two-way ANOVA revealed a main effect of time ($P=0.041$), but Šídák's multiple comparisons test did not show any significant differences timepoints within any treatment group. Mean and standard deviation of left foot faults at each timepoint are shown in Table 11. When left foot faults were normalized to baseline, as shown in Figure 6D, two-way ANOVA revealed no main effects. Mean and standard deviation of left foot

faults normalized to baseline for each group at each timepoint are shown in Table 12. In Figure 7, we investigated the correlation between stroke surface area at 6 weeks post-stroke and Tapered Beam task performance at the earliest recorded timepoint, 1 week post-stroke. No significant correlation was found between stroke surface area and total foot faults (Figure 7A, $P=0.4941$), left foot faults (7B, $P=0.2983$), total foot faults normalized to baseline (7C, $P=0.1254$), or left foot faults normalized to baseline (7D, $P=0.3669$).

For the animals from the two stroke groups assessed in the String Pull task, their task measured were plotted against stroke surface area to investigate the relationship between stroke size and task performance. Figure 8A shows body angle during string pulling at 1 week post-stroke versus stroke surface area at 6 weeks post-stroke. A significant bivariate correlation was observed between these two variables, with $P=0.0338$ and $R^2=0.4498$. Figure 8B shows bimanual coordination during string pulling at 1 week post-stroke versus stroke surface area at 6 weeks post-stroke. No significant bivariate correlation was observed ($P=0.7315$, $R^2=0.01554$). Figure 7C shows left hand Y-reach during string pulling at 1 week post-stroke versus stroke surface area at 6 weeks post-stroke. No significant bivariate correlation was observed ($P=0.5811$, $R^2=0.03969$).

5.4 Visualization of PTN at injection sites

ImageJ software was used to calculate mean gray value of images of PTN immunohistochemistry at regions targeted for cortical microinjection of PTN. These measures were normalized against mean gray value of the contralesional cortex to obtain mean fluorescence intensity of PTN. The three measures of mean fluorescence intensity were averaged for each animal. Immunohistochemistry of PTN was used as an indicator of the presence of PTN protein in brain tissue. Figure 9A shows the mean fluorescence intensity of PTN in naive animals and at 3

and 14 days post-stroke for both PBS- and PTN-treated animals. Ordinary one-way ANOVA revealed no main effect ($P=0.313$), so posthocs were not performed. Figures 8B-F show representative images of PTN (green) and DAPI (blue) images from each investigated experimental group. PTN is expressed by cells in peri-infarct cortex, and this may reduce the sensitivity of intensity measures. Qualitative assessment of PTN immunohistochemistry suggests greater parenchymal (extracellular) labeling in PTN injected animals relative to PBS controls, potentially reflecting PTN from injection.

5.5 Iba1 and GFAP fluorescence were pronounced following stroke, but unaffected by treatment

ImageJ software was used to calculate mean gray value of images of Iba1, a marker of reactive microglia, and GFAP, a marker of reactive astrocytes, immunohistochemistry at regions targeted for cortical microinjection of PTN. These measures were normalized against mean gray value of the contralesional cortex to obtain mean fluorescence intensity of Iba1 and GFAP. The three measures of mean fluorescence intensity were averaged for each animal. Figure 10A shows the mean fluorescence intensity of Iba1 in naive animals and at 3, 7, and 14 days post-stroke for both PBS- and PTN-treated animals. Kruskal-Wallis test revealed a main effect ($P<0.001$). Dunn's multiple comparisons test showed a significant difference between Naive and 7dps-PBS groups ($p<0.001$) and Naive and 7dps-PTN groups ($p=0.001$). Figure 10B shows the mean fluorescence intensity of GFAP in naive and 3, 7, and 14 days post-stroke for both PBS- and PTN-treated animals. Kruskal-Wallis test revealed a main effect ($P=0.002$). Dunn's multiple comparisons test showed a significant difference between Naive and 3dps-PBS groups ($p=0.022$), Naive and 3dps-PTN groups ($p=0.025$), Naive and 7dps-PBS groups ($p=0.046$), and Naive and 7dps-PTN groups

($p=0.007$). Figures 9C-I show representative images of Iba1 (red) and GFAP (green) for each investigated experimental group.

Additionally, ImageJ software was used to conduct cell counts of Iba1-positive (Iba1+) cells on randomly selected animals at 7 days post-stroke and naive animals (Figure 11). Cell counts in the ipsilesional cortex were normalized to cell counts of the contralesional cortex for all animals, and the data points visible in Figure 11A are means of the cell counts at each of the injection sites. Kruskal-Wallis test revealed a main effect ($P=0.0141$). Dunn's multiple comparisons test showed a significant difference between Naive and the PTN treatment group ($p=0.0275$), but no other groups. Figure 11B-D shows representative images of Iba1 fluorescence for each investigated experimental group.

5.6 Myelination is not clearly altered by PTN

ImageJ software was used to calculate mean gray value of images of MBP and O4 immunohistochemistry at regions targeted for cortical microinjection of PTN. MBP is commonly found in the myelin sheath and expressed by mature oligodendrocytes, while O4 is expressed in immature oligodendrocytes. These measures were normalized against mean gray value of the contralesional cortex to obtain mean fluorescence intensity of MBP and O4. The three measures of mean fluorescence intensity were averaged for each animal. Figure 12A shows the mean fluorescence intensity of MBP in naive animals and at 3, 7, and 14 days post-stroke for both PBS- and PTN-treated animals. Kruskal-Wallis test revealed no main effect ($P=0.218$). Figures 12B-H show representative images of MBP (green) for each investigated experimental group. Figure 13A shows the mean fluorescence intensity of O4 in naive animals and at 3, 7, and 14 days post-stroke for both PBS- and PTN-treated animals. Kruskal-Wallis test revealed a main effect ($P=0.023$).

Dunn's multiple comparisons test showed a significant difference between Naive and 3dps-PBS groups ($p=0.021$). Figures 13B-H show representative images of O4 (green) for each investigated experimental group.

6. Discussion

Most functional recovery from stroke occurs in the first 3 months in humans (Nakayama et al., 1994; Wade et al., 1983) and in rodents, much of the recovery occurs within the first few weeks (Krakauer et al., 2012). Rodent models of photothrombosis are characterized by a pronounced glial response in the first few days following infarct and functional deficits specific to the targeted region (Jablonka et al., 2010; H. Li et al., 2014; Shanina et al., 2006; Uzdensky, 2018). In this study, we sought to determine if PTN microinjections delivered to the cortex during the acute phase of stroke recovery could assist functional recovery of deficits associated with the sensorimotor forelimb and hindlimb cortex and influence glial physiology in the ischemic brain.

6.1 Tapered Beam task and String Pull task measures detect minimal functional deficits due to photothrombosis targeted via stereotaxic coordinates

Investigation of brain tissue post-mortem revealed clear infarcts that remained visible 6 weeks after stroke induction (Figure 4). No visible injury was observed at cortical microinjection sites in stroke or sham groups. Treatment did not affect stroke size at endpoint. Despite the presence of clear infarcts, there were no significant functional deficits observed in Tapered Beam (Figure 5B-E) or String Pull (Figure 5F-H) task measures. Additionally, there were no significant differences in task performance between injured animals of different treatment groups. Selecting the animals with the largest strokes and comparing them to naive animals also did not reveal clear deficits in Tapered Beam task performance (Figure 6) and plotting task performance against stroke surface area (Figure 7) also did not reveal any correlation between infarct size and functional performance. Investigating the relationship between stroke size and String Pull task performance, however, did reveal a negative correlation between body angle during string pulling and stroke

size (Figure 8A), where animals with larger strokes displayed a smaller body angle during string pulling motion. Bimanual coordination and the vertical distance travelled by the left hand during reaching showed no relation to stroke size (Figure 8B-C).

This data suggests that the chosen tasks are not sensitive enough for the specific injury model used. It is possible that the targeting of forelimb and hindlimb associated sensorimotor cortex might influence deficits. Here, stereotaxic coordinates were used to target forelimb and hindlimb sensorimotor cortex, and these coordinates may not account for individual subject variation in brain mapping. A more specific method of targeting the forelimb and hindlimb sensorimotor cortex, such as sensory evoked intrinsic signal mapping, could be better suited to these behavioural tests. Unpublished data from the Winship lab identifies transient deficits (1-2 weeks post-stroke) in the Tapered Beam Task in mice when forelimb sensorimotor cortex was first visualized with somatosensory evoked intrinsic imaging and then targeted for infarction (Bandet & Winship, unpublished data). Finally, reduced performance on the Tapered Beam task could be masked by intact locomotor networks, as subcortical motor networks responsible for this function (Darmohray et al., 2019; Han et al., 2013; Muzzu et al., 2018; Saleem et al., 2013) remained uninjured in our model. Notably, the use of this Tapered Beam task in photothrombosis has not been pursued on a timescale this large, but only up to 7 days post-stroke, with deficits being detected in mice with photothrombosis up to 6 days post-stroke (Ardesch et al., 2017). Similarly, in rat models of stroke, the Tapered Beam task has elucidated the most notable deficits up to 1 week post-stroke (Karthikeyan et al., 2019; Obermeyer et al., 2019; Schaar et al., 2010). The String Pull task has also been largely explored in rat models of stroke, where measures such as bimanual coordination and reaching distance of the injured paw deficits within the first week of injury (Blackwell, Köppen, et al., 2018; Blackwell, Widick, et al., 2018). Given the current literature, the

results we observed in our mouse subjects reinforce the need for a larger or more focused infarct, as well as further characterization of these tasks in mice. In line with the literature, the observed significant main effects in Tapered Beam task measures and a significant correlation between body angle during string pulling and stroke size suggest that the use of these tasks in assessing stroke injury is worth continued investigation. For the purposes of this study, the tasks were not sensitive enough to our injury model to conclude whether PTN cortical injection improves functional recovery post-stroke.

6.2 Cortical microinjection of PTN resulted in notable extracellular parenchymal expression of PTN in the ipsilesional cortex

To determine the effectiveness of our PTN administration method, we sought to characterize PTN protein expression post-stroke in animals that received PTN treatment and animals that received vehicle (PBS) treatment. Immunohistochemistry was used to label PTN protein in the cortex and a DAPI stain was used to identify cell nuclei. No statistically significant variation in PTN fluorescence intensity was observed among the selected timepoints, though images and graphs suggest a larger sample size may have confirmed higher PTN levels injected in tissue (Figure 9A). Imaging of PTN showed a cytosolic expression around cell nuclei, especially at 3 days post-stroke, in both PBS and PTN animals (Figure 9B, E). Though the mean fluorescence intensity was slightly more pronounced in PTN groups at both 3 and 14 days post-stroke, this was not a significant difference. An increased fluorescent signal around cells suggests increased PTN in the extracellular parenchyma, which could reflect PTN binding to CSPGs. However, the lack of a clear PTN signal could suggest that our dosage of PTN is not strong enough or that our antibody does not label PTN in tissue. Our highest dosage was 5 mg/ml, whereas some studies have used

dosages as large as 10 mg/ml PTN for cortical microinjections (Paveliev et al., 2016). Another factor could be the timing of PTN injection. Existing literature supports that the presence of endogenous PTN protein and *Ptn* mRNA following ischemic stroke in a rat model is pronounced at 3 and 7 days post-stroke, but diminished by day 14 (Yeh et al., 1998). Likewise, other investigations in our lab have found that post-stroke PTN protein levels are most pronounced at 7 days post-injury (Munchrath & Winship, unpublished data). Elevated endogenous expression may mask PTN signal due to injection. Additionally, a better timepoint for encouraging sustained elevation of PTN in the ischemic cortex may be at day 7, when PTN levels start to drop off, instead of at day 2, when they are just starting to rise. Finally, a method more suited to quantification, such as Western blotting, may more accurately relate injection dose to PTN protein levels in cortical tissue.

6.3 Markers of glial reactivity were not significantly altered in the presence of exogenous PTN

Microglia and astrocyte activity following ischemic stroke has been widely studied and characterized in many injury models, including photothrombosis. Additionally, the effects of PTN on microglia have been documented. Notably, *in vitro* PTN regulates microglial proliferation and enhances phagocytic activity in response to LPS-induced inflammation and oxygen deprivation (Fernández-Calle et al., 2017; Miao et al., 2012), while transgenic studies show that PTN enhances the inflammatory response of microglia by its inhibition of RPTP-beta/zeta (Fernández-Calle et al., 2020). The administration of exogenous PTN and its effects on microglia have also been investigated, particularly in a mouse model of multiple sclerosis (MS) where PTN increased cytokine expression by different microglial subtypes (Miao et al., 2019), and in SCI and brain prick injury model in mice, where PTN administration improved neurite outgrowth and dendritic

sprouting (Paveliev et al., 2016). Microglia are also known to express PTN in animal models of CNS injury (Fernández-Calle et al., 2018; Kaspiris et al., 2016; X. Liu et al., 1998; Yeh et al., 1998). While the effects of PTN on astrocytes have been less explored, current literature suggests that PTN attenuates the reactivity of astrocytes in the presence of inflammation (Fernández-Calle et al., 2017) and that astrocyte-derived PTN is an important regulator of inflammation and regeneration in CNS injury (Iseki et al., 2002; Linnerbauer et al., 2022).

Here, at 7 days post-stroke, Iba1 fluorescence was enhanced in both treatment groups when compared to naive animals; however, there was no variation in Iba1 fluorescence intensity between treatment groups at any timepoint (Figure 10A). In naive brains, Iba1 shows a typical unreactive morphology of microglia, with minimal processes and small cell bodies. From 3 to 7 days post-stroke, Iba1⁺ cells begin to show a swelled morphology with multiple extensive processes, and by 14 days post-stroke Iba1⁺ cells return to a state more similar to the expression seen in naive brains. This aligns with the acute immune response observed in photothrombosis (H. Li et al., 2014). Representative images of this morphology can be seen in Figures 9C-I where Iba1 is shown in red. The effects of PTN on astrocytes have not been investigated to the best of our knowledge. At 3 and 7 days post-stroke, GFAP fluorescence was enhanced in both treatment groups when compared to naive animals; however, there was no variation in GFAP fluorescence intensity between treatment groups at any timepoint (Figure 10B). GFAP is typically used as a marker of reactive astrocytes observed to participate in glial scar formation in ischemic stroke (Silver & Miller, 2004). In naive brains, GFAP expression is very minimal with only a few short processes appearing. GFAP expression is most pronounced at 3 days post-stroke as the glial scar is forming around the damaged brain tissue. Expression is sustained at 7 days post-stroke. At these timepoints, GFAP⁺ cells have visible cell bodies with extensive processes. At 14 days post-stroke, the

presence of GFAP+ cells is diminished, though the expression still shows some pronounced cell bodies with numerous processes instead of the non-reactive state observed in naive brains. This progression of astrocytic morphology was seen in both PBS- and PTN-treated animals, suggesting that post-stroke astrogliosis is not affected by our treatment model.

This data suggests that typical glial density and morphology are unaffected by our administration of PTN, at least in these immunoassays. Given established effects of PTN on glial cells *in vitro* and in a variety of injury models (Fernández-Calle et al., 2017; Iseki et al., 2002; Kaspiris et al., 2016; Linnerbauer et al., 2022; X. Liu et al., 1998; Miao et al., 2012, 2019; Yeh et al., 1998), a more sensitive assessment of glial cell activation via transcriptomics on isolated brain tissue or *in situ* hybridization may be warranted. Moreover, PTN alters cytokine release from microglia, and this may happen without apparent density or morphological changes (Fernández-Calle et al., 2017; Miao et al., 2012, 2019). Additionally, neurons are known to widely express PTN (Wanaka et al., 1993; Yeh et al., 1998) and exhibit neurite outgrowth and regeneration in the presence of PTN (González-Castillo et al., 2015; Gupta et al., 2022; Hida et al., 2003; Taravini et al., 2011). Glial cells play a significant role in dictating neuron survival and regeneration in CNS injury (Y. Chen et al., 2001; Z. Liu & Chopp, 2016; Oshima et al., 2009; Patterson, 2015; Silver & Miller, 2004; Xu et al., 2020); however, it would be of interest to determine whether the trophic effects of PTN can directly enhance neuronal outcomes. Investigating measures such as neuron density or mature neuron cell counts would serve to elucidate the trophic effects of PTN on neurons and their progenitors.

6.4 Markers of OPCs were elevated after stroke, but myelination markers remained stable

PTN has been observed to affect the proliferation of OPCs and myelination (McClain et al., 2012; Reyes-Mata et al., 2021). Through increased phosphorylation of RPTP-zeta, PTN is associated with an increased number of OPCs available for differentiation (Kuboyama et al., 2015, 2016; McClain et al., 2012; Tanga et al., 2019). Exogenous administration of PTN is associated with increased expression of mature oligodendrocyte markers (Kuboyama et al., 2017) and both oligodendrocyte-derived PTN and exogenous PTN promote further oligodendrocyte differentiation (Z. Liu et al., 2022).

By observing O4 and MBP expression, we can visualize post-stroke oligodendrocyte differentiation in the presence of PTN treatment. In the present study, no significant changes in mean fluorescence intensity of MBP were observed (Figure 12A). MBP levels remained relatively stable and expression patterns appeared similar throughout experimental groups. MBP⁺ processes appear encircle cell body-like structures, which can be seen as circular gaps in MBP expression. Representative images of this are available in Figure 12B-H. Furthermore, O4 expression was significantly elevated at 3 days post-stroke but not at any other timepoint or between any treatment groups (Figure 13A). O4 expression appeared to take on a punctate cytosolic pattern, particularly visible in naive brains (Figure 13E). This data suggests that the investigated treatment did not have pronounced effects on oligodendrocyte activity or differentiation in the post-stroke brain. Further investigating O4 expression through other quantification methods, such as cell counting, would be more informative, especially since the role of PTN in OPC proliferation has been well-documented. Additionally, investigating markers of OPCs, such as platelet-derived growth factor receptor alpha (PDGFR-alpha) (Wilson et al., 2006), and mature oligodendrocytes, such as myelin-oligodendrocyte glycoprotein (MOG) (Scolding et al., 1989), for cell counting could better inform

us on oligodendrocyte maturation and differentiation post-stroke and in the presence of PTN. We could also pursue in vivo measures of oligodendrocyte myelination, such as spectral confocal reflectance microscopy (SCoRe), which is a label-free method that would allow for imaging of myelination throughout stroke recovery (Hill et al., 2018; Schain et al., 2014). However, the above data could also suggest investigating a more promising timepoint for PTN administration, such as 7 days post-stroke as mentioned above.

7. Conclusion

Stroke is a leading cause of disability and third leading cause of death in Canada, with the numbers of people living with stroke-related disability only expected to increase over the next decade (Government of Canada, 2017; Krueger et al., 2015). The vast majority of stroke-related disability is characterized by hemiparesis and muscle weakness (Carey, 1995; Kessner et al., 2016). This thesis investigated a therapy with the potential to modulate protective processes in the cortex after ischemic injury, as well as improve functional outcomes.

In this study, we tested the hypothesis that animals administered intracortical injections of PTN would exhibit greater functional recovery in the String Pull and Tapered Beam tests when compared to their baseline performance; enhanced microglial and astrocytic reactivity; and increased expression of O4 and MBP. The cortical microinjections of PTN were targeted to regions surrounding the infarct, which are known to be rich with growth-promoting factors post-stroke and important for functional remapping and spontaneous recovery (Carmichael et al., 2005; Nudo, 2007; Winship & Murphy, 2009). If exogenous PTN can enhance microglial proliferation, astrocyte reactivity, and OPC proliferation, then these are all factors that would serve to protect and reduce further damage to this growth-permissive region during functional recovery. However,

we found that our selected behavioural tests, String Pull and Tapered Beam, did not reveal any treatment effects as they were not sensitive enough for this injury model despite previous reports. For further study, it would be beneficial to use intrinsic imaging to target specific functional regions for infarction and investigate earlier timepoints post-stroke when Tapered Beam and String Pull task outcomes have been clearly identified. To test whether indices of PTN activity in tissue could be detected, immunofluorescent markers were used to examine glial activation and morphology post-stroke. While extracellular parenchymal expression of PTN protein was detectable in the brain, its expression was not significantly affected by treatment at any timepoint following stroke. Additionally, the characterization of glial cells in PTN-treated animals did not significantly vary from that of vehicle-treated animals. There were no clear differences in Iba1 or GFAP expression between treatment groups at any timepoint following stroke; however, conduction of Iba1+ cell counts revealed enhanced proliferation of microglia in the presence of PTN treatment at 7 days post-stroke. Cell counts of remaining timepoints would further elucidate the timescale of this effect. Additionally, cell counts of GFAP+ cells could give a clearer view of astrocyte response to exogenous PTN, which would help fill an existing gap in the literature concerning the effects of PTN on astrocytes in the presence of CNS injury. Further, no clear differences in MBP or O4 expression were detected between treatment groups. As the effects of PTN on oligodendrocyte differentiation in development and injury have been well-documented, more sensitive measures of these markers should be explored. This would include quantifying markers of different timepoints of oligodendrocyte development, namely PDGFR-alpha and MOG, and using SCoRe imaging to quantify post-stroke myelination in response to PTN treatment *in vivo*. Finally, as this data suggests that our periinfarct injections were not having dramatic effects on glial activation in our regions of interest, administering PTN at a later timepoint, such as 7 days

post-stroke, may have a greater effect on the availability of PTN as it would align with the natural decrease in endogenous PTN expression post-stroke.

In this present study, while our injury model produced visible strokes and animals showed typical stroke pathophysiology, we did not observe clear deficits in behaviour or any effect of cortical microinjections of PTN on expression of glial markers or quantifiable availability of PTN protein. We have identified areas for further investigation and potential improvements upon the study design which may help us further elucidate the effects of PTN on sensorimotor functional recovery and glial activity in the ischemic brain.

Bibliography

- Adiguzel, A., Arsava, E. M., & Topcuoglu, M. A. (2021). Temporal course of peripheral inflammation markers and indexes following acute ischemic stroke: Prediction of mortality, functional outcome, and stroke-associated pneumonia. *Neurological Research*, *44*(3), 224–231.
- Alia, C., Spalletti, C., Lai, S., Panarese, A., Lamola, G., Bertolucci, F., Vallone, F., Di Garbo, A., Chisari, C., Micera, S., & Caleo, M. (2017). Neuroplastic Changes Following Brain Ischemia and their Contribution to Stroke Recovery: Novel Approaches in Neurorehabilitation. *Frontiers in Cellular Neuroscience*, *11*.
<https://doi.org/10.3389/fncel.2017.00076>
- Alia, C., Spalletti, C., Lai, S., Panarese, A., Micera, S., & Caleo, M. (2016). Reducing GABAA-mediated inhibition improves forelimb motor function after focal cortical stroke in mice. *Scientific Reports*, *6*(1), 37823. <https://doi.org/10.1038/srep37823>
- Allred, R. P., Cappellini, C. H., & Jones, T. A. (2010). The “good” limb makes the “bad” limb worse: Experience-dependent interhemispheric disruption of functional outcome after cortical infarcts in rats. *Behavioral Neuroscience*, *124*(1), 124.
<https://doi.org/10.1037/a0018457>
- Andersen, G., Vestergaard, K., Ingeman-Nielsen, M., & Jensen, T. S. (1995). Incidence of central post-stroke pain. *Pain*, *61*(2), 187–193. [https://doi.org/10.1016/0304-3959\(94\)00144-4](https://doi.org/10.1016/0304-3959(94)00144-4)
- Ardesch, D. J., Balbi, M., & Murphy, T. H. (2017). Automated touch sensing in the mouse tapered beam test using Raspberry Pi. *Journal of Neuroscience Methods*, *291*, 221–226.
<http://dx.doi.org/10.1016/j.jneumeth.2017.08.030>

- Asai, H., Yokoyama, S., Morita, S., Maeda, N., & Miyata, S. (2009). Functional difference of receptor-type protein tyrosine phosphatase ζ/β isoforms in neurogenesis of hippocampal neurons. *Neuroscience*, *164*(3), 1020–1030.
<https://doi.org/10.1016/j.neuroscience.2009.09.012>
- Bao, X., Mikami, T., Yamada, S., Faissner, A., Muramatsu, T., & Sugahara, K. (2005). Heparin-binding Growth Factor, Pleiotrophin, Mediates Neuritogenic Activity of Embryonic Pig Brain-derived Chondroitin Sulfate/Dermatan Sulfate Hybrid Chains. *Journal of Biological Chemistry*, *280*(10), 9180–9191. <https://doi.org/10.1074/jbc.M413423200>
- Barde, Y.-A. (1989). Trophic factors and neuronal survival. *Neuron*, *2*(6), 1525–1534.
[https://doi.org/10.1016/0896-6273\(89\)90040-8](https://doi.org/10.1016/0896-6273(89)90040-8)
- Barritt, A. W., Davies, M., Marchand, F., Hartley, R., Grist, J., Yip, P., McMahon, S. B., & Bradbury, E. J. (2006). Chondroitinase ABC Promotes Sprouting of Intact and Injured Spinal Systems after Spinal Cord Injury. *Journal of Neuroscience*, *26*(42), 10856–10867.
<https://doi.org/10.1523/JNEUROSCI.2980-06.2006>
- Basille-Dugay, M., Hamza, M. M., Tassery, C., Parent, B., Raoult, E., Bénard, M., Raisman-Vozari, R., Vaudry, D., & Burel, D. C. (2013). Spatio-temporal characterization of the pleiotrophinergic system in mouse cerebellum: Evidence for its key role during ontogenesis. *Experimental Neurology*, *247*, 537–551.
<https://doi.org/10.1016/j.expneurol.2013.02.004>
- Benakis, C., Garcia-Bonilla, L., Iadecola, C., & Anrather, J. (2015). The role of microglia and myeloid immune cells in acute cerebral ischemia. *Frontiers in Cellular Neuroscience*, *8*.
<https://doi.org/10.3389/fncel.2014.00461>

- Bernhardt, J., Dewey, H., Collier, J., Thrift, A., Lindley, R., Moodie, M., & Donnan, G. (2006). A Very Early Rehabilitation Trial (AVERT). *International Journal of Stroke*, *1*(3), 169–171. <https://doi.org/10.1111/j.1747-4949.2006.00044.x>
- Biernaskie, J. (2004). Efficacy of Rehabilitative Experience Declines with Time after Focal Ischemic Brain Injury. *Journal of Neuroscience*, *24*(5), Article 5. <https://doi.org/10.1523/JNEUROSCI.3834-03.2004>
- Blackwell, A. A., Banovetz, M. T., Qandeel, Whishaw, I. Q., & Wallace, D. G. (2018). The structure of arm and hand movements in a spontaneous and food rewarded on-line string-pulling task by the mouse. *Behavioural Brain Research*, *345*, 49–58. <https://doi.org/10.1016/j.bbr.2018.02.025>
- Blackwell, A. A., Köppen, J. R., Whishaw, I. Q., & Wallace, D. G. (2018). String-pulling for food by the rat: Assessment of movement, topography and kinematics of a bilaterally skilled forelimb act. *Learning and Motivation*, *61*, 63–73. <https://doi.org/10.1016/j.lmot.2017.03.010>
- Blackwell, A. A., Widick, W. L., Cheatwood, J. L., Whishaw, I. Q., & Wallace, D. G. (2018). Unilateral forelimb sensorimotor cortex devascularization disrupts the topographic and kinematic characteristics of hand movements while string-pulling for food in the rat. *Behavioural Brain Research*, *338*, 88–100. <https://doi.org/10.1016/j.bbr.2017.10.014>
- Blondet, B., Carpentier, G., Lafdil, F., & Courty, J. (2005). Pleiotrophin Cellular Localization in Nerve Regeneration after Peripheral Nerve Injury. *Journal of Histochemistry & Cytochemistry*, *53*(8), Article 8. <https://doi.org/10.1369/jhc.4A6574.2005>
- Bolay, H., Gürsoy-Özdemir, Y., Sara, Y., Onur, R., Can, A., & Dalkara, T. (2002). Persistent Defect in Transmitter Release and Synapsin Phosphorylation in Cerebral Cortex After

- Transient Moderate Ischemic Injury. *Stroke*, 33(5), 1369–1375.
<https://doi.org/10.1161/01.STR.0000013708.54623.DE>
- Bradbury, E. J., Moon, L. D. F., Popat, R. J., King, V. R., Bennett, G. S., Patel, P. N., Fawcett, J. W., & McMahon, S. B. (2002). Chondroitinase ABC promotes functional recovery after spinal cord injury. *Nature*, 416(6881), 636–640. <https://doi.org/10.1038/416636a>
- Brown, C. E., Aminoltejari, K., Erb, H., Winship, I. R., & Murphy, T. H. (2009). In Vivo Voltage-Sensitive Dye Imaging in Adult Mice Reveals That Somatosensory Maps Lost to Stroke Are Replaced over Weeks by New Structural and Functional Circuits with Prolonged Modes of Activation within Both the Peri-Infarct Zone and Distant Sites. *Journal of Neuroscience*, 29(6), 1719–1734. <https://doi.org/10.1523/JNEUROSCI.4249-08.2009>
- Brown, C. E., Li, P., Boyd, J. D., Delaney, K. R., & Murphy, T. H. (2007). Extensive Turnover of Dendritic Spines and Vascular Remodeling in Cortical Tissues Recovering from Stroke. *Journal of Neuroscience*, 27(15), 4101–4109.
<https://doi.org/10.1523/JNEUROSCI.4295-06.2007>
- Butefisch, C. M. (2003). Remote changes in cortical excitability after stroke. *Brain*, 126(2), 470–481. <https://doi.org/10.1093/brain/awg044>
- Byblow, W. D., Stinear, C. M., Barber, P. A., Petoe, M. A., & Ackerley, S. J. (2015). Proportional recovery after stroke depends on corticomotor integrity. *Annals of Neurology*, 78(6), 848–859. <https://doi.org/10.1002/ana.24472>
- Carey, L. M. (1995). Somatosensory Loss after Stroke. *Critical Reviews in Physical and Rehabilitation Medicine*, 7(1), Article 1.
<https://doi.org/10.1615/CritRevPhysRehabilMed.v7.i1.40>

- Carmichael, S. T. (2003). Plasticity of Cortical Projections after Stroke. *The Neuroscientist*, 9(1), 64–75. <https://doi.org/10.1177/1073858402239592>
- Carmichael, S. T. (2006). Cellular and molecular mechanisms of neural repair after stroke: Making waves. *Annals of Neurology*, 59(5), 735–742. <https://doi.org/10.1002/ana.20845>
- Carmichael, S. T., Archibeque, I., Luke, L., Nolan, T., Momiy, J., & Li, S. (2005). Growth-associated gene expression after stroke: Evidence for a growth-promoting region in peri-infarct cortex. *Experimental Neurology*, 193(2), Article 2. <https://doi.org/10.1016/j.expneurol.2005.01.004>
- Carmichael, S. T., & Chesselet, M.-F. (2002). Synchronous Neuronal Activity Is a Signal for Axonal Sprouting after Cortical Lesions in the Adult. *The Journal of Neuroscience*, 22(14), 6062–6070. <https://doi.org/10.1523/JNEUROSCI.22-14-06062.2002>
- Carmichael, S. T., Tatsukawa, K., Katsman, D., Tsuyuguchi, N., & Kornblum, H. I. (2004). Evolution of Diaschisis in a Focal Stroke Model. *Stroke*, 35(3), 758–763. <https://doi.org/10.1161/01.STR.0000117235.11156.55>
- Carter, L. M., McMahon, S. B., & Bradbury, E. J. (2011). Delayed treatment with Chondroitinase ABC reverses chronic atrophy of rubrospinal neurons following spinal cord injury. *Experimental Neurology*, 228(1), Article 1. <https://doi.org/10.1016/j.expneurol.2010.12.023>
- Chamorro, Á., Dirnagl, U., Urra, X., & Planas, A. M. (2016). Neuroprotection in acute stroke: Targeting excitotoxicity, oxidative and nitrosative stress, and inflammation. *The Lancet Neurology*, 15(8), 869–881. [https://doi.org/10.1016/S1474-4422\(16\)00114-9](https://doi.org/10.1016/S1474-4422(16)00114-9)
- Chang, M.-H., Huang, C.-J., Hwang, S.-P. L., Lu, I.-C., Lin, C.-M., Kuo, T.-F., & Chou, C.-M. (2004). Zebrafish heparin-binding neurotrophic factor enhances neurite outgrowth during

- its development. *Biochemical and Biophysical Research Communications*, 321(2), 502–509. <https://doi.org/10.1016/j.bbrc.2004.06.172>
- Chen, X., Liao, S., Ye, L., Gong, Q., Ding, Q., Zeng, J., & Yu, J. (2014). Neuroprotective effect of chondroitinase ABC on primary and secondary brain injury after stroke in hypertensive rats. *Brain Research*, 1543, 324–333. <https://doi.org/10.1016/j.brainres.2013.12.002>
- Chen, Y., Vartiainen, N. E., Ying, W., Chan, P. H., Koistinaho, J., & Swanson, R. A. (2001). Astrocytes protect neurons from nitric oxide toxicity by a glutathione-dependent mechanism: Astrocytes block NO-mediated neurotoxicity. *Journal of Neurochemistry*, 77(6), 1601–1610. <https://doi.org/10.1046/j.1471-4159.2001.00374.x>
- Clarkson, A. N., Overman, J. J., Zhong, S., Mueller, R., Lynch, G., & Carmichael, S. T. (2011). AMPA Receptor-Induced Local Brain-Derived Neurotrophic Factor Signaling Mediates Motor Recovery after Stroke. *Journal of Neuroscience*, 31(10), 3766–3775. <https://doi.org/10.1523/JNEUROSCI.5780-10.2011>
- Cua, R. C., Lau, L. W., Keough, M. B., Midha, R., Apte, S. S., & Yong, V. W. (2013). Overcoming neurite-inhibitory chondroitin sulfate proteoglycans in the astrocyte matrix: Metalloproteinases in axonal regeneration. *Glia*, 61(6), Article 6. <https://doi.org/10.1002/glia.22489>
- Darmohray, D. M., Jacobs, J. R., Marques, H. G., & Carey, M. R. (2019). Spatial and Temporal Locomotor Learning in Mouse Cerebellum. *Neuron*, 102(1), 217-231.e4. <https://doi.org/10.1016/j.neuron.2019.01.038>

- Demyanenko, S., & Uzdensky, A. (2017). Profiling of Signaling Proteins in Penumbra After Focal Photothrombotic Infarct in the Rat Brain Cortex. *Molecular Neurobiology*, 54(9), 6839–6856. <https://doi.org/10.1007/s12035-016-0191-x>
- Dewar, D., Underhill, S. M., & Goldberg, M. P. (2003). Oligodendrocytes and Ischemic Brain Injury. *Journal of Cerebral Blood Flow & Metabolism*, 23(3), 263–274. <https://doi.org/10.1097/01.WCB.0000053472.41007.F9>
- Dijkhuizen, R. M., Ren, J., Mandeville, J. B., Wu, O., Ozdag, F. M., Moskowitz, M. A., Rosen, B. R., & Finklestein, S. P. (2001). Functional magnetic resonance imaging of reorganization in rat brain after stroke. *Proceedings of the National Academy of Sciences*, 98(22), 12766–12771. <https://doi.org/10.1073/pnas.231235598>
- Emsley, H. C. A., Smith, C. J., Tyrrell, P. J., & Hopkins, S. J. (2008). Inflammation in Acute Ischemic Stroke and its Relevance to Stroke Critical Care. *Neurocritical Care*, 9(1), 125–138. <https://doi.org/10.1007/s12028-007-9035-x>
- Endres, M., Dirnagl, U., & Moskowitz, M. A. (2008). Chapter 2 The ischemic cascade and mediators of ischemic injury. In *Handbook of Clinical Neurology* (Vol. 92, pp. 31–41). Elsevier. [https://doi.org/10.1016/S0072-9752\(08\)01902-7](https://doi.org/10.1016/S0072-9752(08)01902-7)
- Farrell, R., Evans, S., & Corbett, D. (2001). Environmental enrichment enhances recovery of function but exacerbates ischemic cell death. *Neuroscience*, 107(4), 585–592. [https://doi.org/10.1016/S0306-4522\(01\)00386-4](https://doi.org/10.1016/S0306-4522(01)00386-4)
- Fawcett, J. W., & Asher, Richard. A. (1999). The glial scar and central nervous system repair. *Brain Research Bulletin*, 49(6), 377–391. [https://doi.org/10.1016/S0361-9230\(99\)00072-](https://doi.org/10.1016/S0361-9230(99)00072-6)

- Feigin, V. L., Brainin, M., Norrving, B., Martins, S., Sacco, R. L., Hacke, W., Fisher, M., Pandian, J., & Lindsay, P. (2022). World Stroke Organization (WSO): Global Stroke Fact Sheet 2022. *International Journal of Stroke*, *17*(1), 18–29.
<https://doi.org/10.1177/17474930211065917>
- Fernández-Calle, R., Galán-Llario, M., Gramage, E., Zapatería, B., Vicente-Rodríguez, M., Zapico, J. M., de Pascual-Teresa, B., Ramos, A., Ramos-Álvarez, M. P., Uribarri, M., Ferrer-Alcón, M., & Herradón, G. (2020). Role of RPTP β/ζ in neuroinflammation and microglia-neuron communication. *Scientific Reports*, *10*(1), 20259.
<https://doi.org/10.1038/s41598-020-76415-5>
- Fernández-Calle, R., Vicente-Rodríguez, M., Gramage, E., de la Torre-Ortiz, C., Pérez-García, C., Ramos, M. P., & Herradón, G. (2018). Endogenous pleiotrophin and midkine regulate LPS-induced glial responses. *Neuroscience Letters*, *662*, 213–218.
<https://doi.org/10.1016/j.neulet.2017.10.038>
- Fernández-Calle, R., Vicente-Rodríguez, M., Gramage, E., Pita, J., Pérez-García, C., Ferrer-Alcón, M., Uribarri, M., Ramos, M. P., & Herradón, G. (2017). Pleiotrophin regulates microglia-mediated neuroinflammation. *Journal of Neuroinflammation*, *14*, 1–10.
<https://doi.org/10.1186/s12974-017-0823-8>
- Fournier, A. E., Beer, J., Arregui, C. O., Essagian, C., Aguayo, A. J., & McKerracher, L. (1997). Brain-derived neurotrophic factor modulates GAP-43 but not τ 1 expression in injured retinal ganglion cells of adult rats. *Journal of Neuroscience Research*, *47*(6), 561–572.
[https://doi.org/10.1002/\(SICI\)1097-4547\(19970315\)47:6<561::AID-JNR1>3.0.CO;2-B](https://doi.org/10.1002/(SICI)1097-4547(19970315)47:6<561::AID-JNR1>3.0.CO;2-B)

- G. Broeks, J., Lankhorst, G. J., Rumping, K., & Prevo, A. J. H. (1999). The long-term outcome of arm function after stroke: Results of a follow-up study. *Disability and Rehabilitation*, *21*(8), 357–364. <https://doi.org/10.1080/096382899297459>
- Gao, T. M., Pulsinelli, W. A., & Xu, Z. C. (1999). Changes in membrane properties of CA1 pyramidal neurons after transient forebrain ischemia in vivo. *Neuroscience*, *90*(3), 771–780. [https://doi.org/10.1016/S0306-4522\(98\)00493-X](https://doi.org/10.1016/S0306-4522(98)00493-X)
- García-Alías, G., Barkhuysen, S., Buckle, M., & Fawcett, J. W. (2009). Chondroitinase ABC treatment opens a window of opportunity for task-specific rehabilitation. *Nature Neuroscience*, *12*(9), Article 9. <https://doi.org/10.1038/nn.2377>
- Geremia, N. M., Pettersson, L. M. E., Hasmatali, J. C., Hryciw, T., Danielsen, N., Schreyer, D. J., & Verge, V. M. K. (2010). Endogenous BDNF regulates induction of intrinsic neuronal growth programs in injured sensory neurons. *Experimental Neurology*, *223*(1), 128–142. <https://doi.org/10.1016/j.expneurol.2009.07.022>
- Gleichman, A. J., & Carmichael, S. T. (2014). Astrocytic therapies for neuronal repair in stroke. *Neuroscience Letters*, *565*, 47–52. <https://doi.org/10.1016/j.neulet.2013.10.055>
- González-Castillo, C., Ortuño-Sahagún, D., Guzmán-Brambila, C., Pallàs, M., & Rojas-Mayorquín, A. E. (2015). Pleiotrophin as a central nervous system neuromodulator, evidences from the hippocampus. *Frontiers in Cellular Neuroscience*, *8*. <https://doi.org/10.3389/fncel.2014.00443>
- Gorup, D., Boháček, I., Miličević, T., Pochet, R., Mitrečić, D., Križ, J., & Gajović, S. (2015). Increased expression and colocalization of GAP43 and CASP3 after brain ischemic lesion in mouse. *Neuroscience Letters*, *597*, 176–182. <https://doi.org/10.1016/j.neulet.2015.04.042>

- Government of Canada. (2017). *Stroke in Canada: Highlights from the Canadian Chronic Disease Surveillance System*. Government of Canada. <https://www.canada.ca/en/public-health/services/publications/diseases-conditions/stroke-canada-fact-sheet.html>
- Green, J. B. (2003). Brain Reorganization After Stroke. *Topics in Stroke Rehabilitation*, 10(3), Article 3. <https://doi.org/10.1310/H65X-23HW-QL1G-KTNQ>
- Greenberg, D. A., & Jin, K. (2006). Growth factors and stroke. *NeuroRX*, 3(4), 458–465. <https://doi.org/10.1016/j.nurx.2006.08.003>
- Gupta, S. J., Churchward, M. A., Todd, K. G., & Winship, I. R. (2022). *Pleiotrophin signals through ALK receptor to enhance growth of neurons in the presence of inhibitory CSPGs* [Preprint]. Neuroscience. <https://doi.org/10.1101/2022.04.01.486745>
- Hacke, W. (1995). Intravenous thrombolysis with recombinant tissue plasminogen activator for acute hemispheric stroke. The European Cooperative Acute Stroke Study (ECASS). *JAMA: The Journal of the American Medical Association*, 274(13), 1017–1025. <https://doi.org/10.1001/jama.274.13.1017>
- Hakkoum, D., Stoppini, L., & Muller, D. (2007). Interleukin-6 promotes sprouting and functional recovery in lesioned organotypic hippocampal slice cultures. *Journal of Neurochemistry*, 100(3), 747–757. <https://doi.org/10.1111/j.1471-4159.2006.04257.x>
- Han, Q., Feng, J., Qu, Y., Ding, Y., Wang, M., So, K.-F., Wu, W., & Zhou, L. (2013). Spinal cord maturation and locomotion in mice with an isolated cortex. *Neuroscience*, 253, 235–244. <https://doi.org/10.1016/j.neuroscience.2013.08.057>
- Hara, Y. (2015). Brain Plasticity and Rehabilitation in Stroke Patients. *Journal of Nippon Medical School*, 82(1), Article 1. <https://doi.org/10.1272/jnms.82.4>

- Hawe, R. L., Scott, S. H., & Dukelow, S. P. (2019). Taking Proportional Out of Stroke Recovery. *Stroke*, *50*(1), 204–211. <https://doi.org/10.1161/STROKEAHA.118.023006>
- Hida, H., Jung, C.-G., Wu, C.-Z., Kim, H.-J., Kodama, Y., Masuda, T., & Nishino, H. (2003). Pleiotrophin exhibits a trophic effect on survival of dopaminergic neurons in vitro. *European Journal of Neuroscience*, *17*(10), 2127–2134. <https://doi.org/10.1046/j.1460-9568.2003.02661.x>
- Hill, R. A., Li, A. M., & Grutzendler, J. (2018). Lifelong cortical myelin plasticity and age-related degeneration in the live mammalian brain. *Nature Neuroscience*, *21*(5), 683–695. <https://doi.org/10.1038/s41593-018-0120-6>
- Hosp, J. A., & Luft, A. R. (2011). Cortical Plasticity during Motor Learning and Recovery after Ischemic Stroke. *Neural Plasticity*, *2011*, 1–9. <https://doi.org/10.1155/2011/871296>
- Hossmann, K.-A. (2006). Pathophysiology and Therapy of Experimental Stroke. *Cellular and Molecular Neurobiology*, *26*(7–8), 1055–1081. <https://doi.org/10.1007/s10571-006-9008-1>
- Hu, J., Liu, P.-L., Hua, Y., Gao, B.-Y., Wang, Y.-Y., Bai, Y.-L., & Chen, C. (2021). Constraint-induced movement therapy enhances AMPA receptor-dependent synaptic plasticity in the ipsilateral hemisphere following ischemic stroke. *Neural Regeneration Research*, *16*(2), 319. <https://doi.org/10.4103/1673-5374.290900>
- Huang, J., Upadhyay, U. M., & Tamargo, R. J. (2006). Inflammation in stroke and focal cerebral ischemia. *Surgical Neurology*, *66*(3), Article 3. <https://doi.org/10.1016/j.surneu.2005.12.028>

- Huang, L., Wu, Z.-B., ZhuGe, Q., Zheng, W., Shao, B., Wang, B., Sun, F., & Jin, K. (2014). Glial Scar Formation Occurs in the Human Brain after Ischemic Stroke. *International Journal of Medical Sciences*, *11*(4), 344–348. <https://doi.org/10.7150/ijms.8140>
- Hummel, F. C., & Cohen, L. G. (2006). Non-invasive brain stimulation: A new strategy to improve neurorehabilitation after stroke? *The Lancet Neurology*, *5*(8), 708–712. [https://doi.org/10.1016/S1474-4422\(06\)70525-7](https://doi.org/10.1016/S1474-4422(06)70525-7)
- Hummel, F., & Cohen, L. G. (2005). Improvement of Motor Function with Noninvasive Cortical Stimulation in a Patient with Chronic Stroke. *Neurorehabilitation and Neural Repair*, *19*(1), 14–19. <https://doi.org/10.1177/1545968304272698>
- Inayat, S., Singh, S., Ghasroddashti, A., Qandeel, Egodage, P., Whishaw, I. Q., & Mohajerani, M. H. (2020). A Matlab-based toolbox for characterizing behavior of rodents engaged in string-pulling. *ELife*, *9*, e54540. <https://doi.org/10.7554/eLife.54540>
- Iseki, K., Hagino, S., Mori, T., Zhang, Y., Yokoya, S., Takaki, H., Tase, C., Murakawa, M., & Wanaka, A. (2002). Increased syndecan expression by pleiotrophin and FGF receptor-expressing astrocytes in injured brain tissue. *Glia*, *39*(1), 1–9. <https://doi.org/10.1002/glia.10078>
- Ito, D., Tanaka, K., Suzuki, S., Dembo, T., & Fukuuchi, Y. (2001). Enhanced Expression of Iba1, Ionized Calcium-Binding Adapter Molecule 1, After Transient Focal Cerebral Ischemia In Rat Brain. *Stroke*, *32*(5), Article 5. <https://doi.org/10.1161/01.STR.32.5.1208>
- Jablonka, J. A., Burnat, K., Witte, O. W., & Kossut, M. (2010). Remapping of the somatosensory cortex after a photothrombotic stroke: Dynamics of the compensatory reorganization. *Neuroscience*, *165*(1), 90–100. <https://doi.org/10.1016/j.neuroscience.2009.09.074>

- Jacobs, K., & Donoghue, J. (1991). Reshaping the cortical motor map by unmasking latent intracortical connections. *Science*, *251*(4996), 944–947.
<https://doi.org/10.1126/science.2000496>
- Kadomatsu, K., & Muramatsu, T. (2004). Midkine and pleiotrophin in neural development and cancer. *Cancer Letters*, *204*(2), 127–143. [https://doi.org/10.1016/S0304-3835\(03\)00450-6](https://doi.org/10.1016/S0304-3835(03)00450-6)
- Karthikeyan, S., Jeffers, M. S., Carter, A., & Corbett, D. (2019). Characterizing Spontaneous Motor Recovery Following Cortical and Subcortical Stroke in the Rat. *Neurorehabilitation and Neural Repair*, *33*(1), 27–37.
<https://doi.org/10.1177/1545968318817823>
- Kaspiris, A., Chronopoulos, E., Grivas, T. B., Vasiliadis, E., Khaldi, L., Lamprou, M., Lelovas, P. P., Papaioannou, N., Dontas, I. A., & Papadimitriou, E. (2016). Effects of mechanical loading on the expression of pleiotrophin and its receptor protein tyrosine phosphatase beta/zeta in a rat spinal deformity model. *Cytokine*, *78*, 7–15.
<https://doi.org/10.1016/j.cyto.2015.11.017>
- Kerr, A. L., Cheng, S.-Y., & Jones, T. A. (2011). Experience-dependent neural plasticity in the adult damaged brain. *Journal of Communication Disorders*, S0021992411000335.
<https://doi.org/10.1016/j.jcomdis.2011.04.011>
- Kessner, S. S., Bingel, U., & Thomalla, G. (2016). Somatosensory deficits after stroke: A scoping review. *Topics in Stroke Rehabilitation*, *23*(2), Article 2.
<https://doi.org/10.1080/10749357.2015.1116822>

- Kleim, J. A. (2011). Neural plasticity and neurorehabilitation: Teaching the new brain old tricks. *Journal of Communication Disorders, 44*(5), 521–528.
<https://doi.org/10.1016/j.jcomdis.2011.04.006>
- Kobayashi, N. R., Fan, D.-P., Giehl, K. M., Bedard, A. M., Wiegand, S. J., & Tetzlaff, W. (n.d.). *BDNF and NT-4/5 Prevent Atrophy of Rat Rubrospinal Neurons after Cervical Axotomy, Stimulate GAP-43 and T₁-Tubulin mRNA Expression, and Promote Axonal Regeneration*. 13.
- Kolosowska, N., Keuters, M. H., Wojciechowski, S., Keksa-Goldsteine, V., Laine, M., Malm, T., Goldsteins, G., Koistinaho, J., & Dhungana, H. (2019). Peripheral Administration of IL-13 Induces Anti-inflammatory Microglial/Macrophage Responses and Provides Neuroprotection in Ischemic Stroke. *Neurotherapeutics, 16*(4), 1304–1319.
<https://doi.org/10.1007/s13311-019-00761-0>
- Kozlowski, D. A., James, D. C., & Schallert, T. (1996). *Use-Dependent Exaggeration of Neuronal Injury after Unilateral Sensorimotor Cortex Lesions*. *16*(15), 4776–4786.
- Krakauer, J. W., Carmichael, S. T., Corbett, D., & Wittenberg, G. F. (2012). Getting Neurorehabilitation Right: What Can Be Learned From Animal Models? *Neurorehabilitation and Neural Repair, 26*(8), Article 8.
<https://doi.org/10.1177/1545968312440745>
- Kreisel, S. H., Bänzner, H., & Hennerici, M. G. (2006). Pathophysiology of Stroke Rehabilitation: Temporal Aspects of Neurofunctional Recovery. *Cerebrovascular Diseases, 21*(1–2), 6–17. <https://doi.org/10.1159/000089588>

- Krueger, H., Koot, J., Hall, R. E., O'Callaghan, C., Bayley, M., & Corbett, D. (2015). Prevalence of Individuals Experiencing the Effects of Stroke in Canada. *Stroke*, *46*(8), 2226–2231. <https://doi.org/10.1161/STROKEAHA.115.009616>
- Kuboyama, K., Fujikawa, A., Suzuki, R., & Noda, M. (2015). Inactivation of Protein Tyrosine Phosphatase Receptor Type Z by Pleiotrophin Promotes Remyelination through Activation of Differentiation of Oligodendrocyte Precursor Cells. *Journal of Neuroscience*, *35*(35), 12162–12171. <https://doi.org/10.1523/JNEUROSCI.2127-15.2015>
- Kuboyama, K., Fujikawa, A., Suzuki, R., Tanga, N., & Noda, M. (2016). Role of Chondroitin Sulfate (CS) Modification in the Regulation of Protein-tyrosine Phosphatase Receptor Type Z (PTPRZ) Activity. *Journal of Biological Chemistry*, *291*(35), 18117–18128. <https://doi.org/10.1074/jbc.M116.742536>
- Kuboyama, K., Tanga, N., Suzuki, R., Fujikawa, A., & Noda, M. (2017). Protamine neutralizes chondroitin sulfate proteoglycan-mediated inhibition of oligodendrocyte differentiation. *PLOS ONE*, *12*(12), e0189164. <https://doi.org/10.1371/journal.pone.0189164>
- Kundert, R., Goldsmith, J., Veerbeek, J. M., Krakauer, J. W., & Luft, A. R. (2019). What the Proportional Recovery Rule Is (and Is Not): Methodological and Statistical Considerations. *Neurorehabilitation and Neural Repair*, *33*(11), 876–887. <https://doi.org/10.1177/1545968319872996>
- Langhorne, P., Stott, D., Knight, A., Bernhardt, J., Barer, D., & Watkins, C. (2010). Very Early Rehabilitation or Intensive Telemetry after Stroke: A Pilot Randomised Trial. *Cerebrovascular Diseases*, *29*(4), Article 4. <https://doi.org/10.1159/000278931>
- Langhorne, P., Wu, O., Rodgers, H., Ashburn, A., & Bernhardt, J. (2017). A Very Early Rehabilitation Trial after stroke (AVERT): A Phase III, multicentre, randomised

- controlled trial. *Health Technology Assessment*, 21(54), 1–120.
<https://doi.org/10.3310/hta21540>
- Lee, H., McKeon, R. J., & Bellamkonda, R. V. (2010). Sustained delivery of thermostabilized chABC enhances axonal sprouting and functional recovery after spinal cord injury. *Proceedings of the National Academy of Sciences*, 107(8), Article 8.
<https://doi.org/10.1073/pnas.09054371106>
- Lee, T.-H., Kato, H., Chen, S.-T., Kogure, K., & Itoyama, Y. (1998). Expression of Nerve Growth Factor and trkA After Transient Focal Cerebral Ischemia in Rats. *Stroke*, 29(8), 1687–1697. <https://doi.org/10.1161/01.STR.29.8.1687>
- Levy, C. E., Nichols, D. S., Schmalbrock, P. M., Keller, P., & Chakeres, D. W. (2001). Functional MRI Evidence of Cortical Reorganization in Upper-Limb Stroke Hemiplegia Treated with Constraint-Induced Movement Therapy: *American Journal of Physical Medicine & Rehabilitation*, 80(1), 4–12. <https://doi.org/10.1097/00002060-200101000-00003>
- Li, C.-X., & Waters, R. S. (1991). Organization of the Mouse Motor Cortex Studied by Retrograde Tracing and Intracortical Microstimulation (ICMS) Mapping. *Canadian Journal of Neurological Sciences / Journal Canadien Des Sciences Neurologiques*, 18(1), 28–38. <https://doi.org/10.1017/S0317167100031267>
- Li, H., Zhang, N., Lin, H.-Y., Yu, Y., Cai, Q.-Y., Ma, L., & Ding, S. (2014). Histological, cellular and behavioral assessments of stroke outcomes after photothrombosis-induced ischemia in adult mice. *BMC Neuroscience*, 15(1), 58. <https://doi.org/10.1186/1471-2202-15-58>

- Li, S., & Carmichael, S. T. (2006). Growth-associated gene and protein expression in the region of axonal sprouting in the aged brain after stroke. *Neurobiology of Disease*, *23*(2), 362–373. <https://doi.org/10.1016/j.nbd.2006.03.011>
- Liepert, J., Bauder, H., Miltner, W. H. R., Taub, E., & Weiller, C. (2000). Treatment-Induced Cortical Reorganization After Stroke in Humans. *Stroke*, *31*(6), 1210–1216. <https://doi.org/10.1161/01.STR.31.6.1210>
- Liepert, J., Miltner, W. H. R., Bauder, H., Sommer, M., Dettmers, C., Taub, E., & Weiller, C. (1998). Motor cortex plasticity during constraint-induced movement therapy in stroke patients. *Neuroscience Letters*, *250*(1), 5–8. [https://doi.org/10.1016/S0304-3940\(98\)00386-3](https://doi.org/10.1016/S0304-3940(98)00386-3)
- Linnerbauer, M., Lößlein, L., Farrenkopf, D., Vandrey, O., Tsaktanis, T., Naumann, U., & Rothhammer, V. (2022). Astrocyte-Derived Pleiotrophin Mitigates Late-Stage Autoimmune CNS Inflammation. *Frontiers in Immunology*, *12*, 800128. <https://doi.org/10.3389/fimmu.2021.800128>
- Liu, X., Mashour, G. A., Webster, H. D., & Kurtz, A. (1998). Basic FGF and FGF receptor 1 are expressed in microglia during experimental autoimmune encephalomyelitis: Temporally distinct expression of midkine and pleiotrophin. *Glia*, *24*(4), 390–397. [https://doi.org/10.1002/\(SICI\)1098-1136\(199812\)24:4<390::AID-GLIA4>3.0.CO;2-1](https://doi.org/10.1002/(SICI)1098-1136(199812)24:4<390::AID-GLIA4>3.0.CO;2-1)
- Liu, Z., & Chopp, M. (2016). Astrocytes, therapeutic targets for neuroprotection and neurorestoration in ischemic stroke. *Progress in Neurobiology*, *144*, 103–120. <https://doi.org/10.1016/j.pneurobio.2015.09.008>
- Liu, Z., Yan, M., Lei, W., Jiang, R., Dai, W., Chen, J., Wang, C., Li, L., Wu, M., Nian, X., Li, D., Sun, D., Lv, X., Wang, C., Xie, C., Yao, L., Wu, C., Hu, J., Xiao, N., ... Zhang, L.

- (2022). Sec13 promotes oligodendrocyte differentiation and myelin repair through autocrine pleiotrophin signaling. *Journal of Clinical Investigation*, 132(7), e155096. <https://doi.org/10.1172/JCI155096>
- Luan, X., Qiu, H., Hong, X., Wu, C., Zhao, K., Chen, H., Zhu, Z., Li, X., Shen, H., & He, J. (2019). High serum nerve growth factor concentrations are associated with good functional outcome at 3 months following acute ischemic stroke. *Clinica Chimica Acta*, 488, 20–24. <https://doi.org/10.1016/j.cca.2018.10.030>
- McClain, C. R., Sim, F. J., & Goldman, S. A. (2012). Pleiotrophin Suppression of Receptor Protein Tyrosine Phosphatase Maintains the Self-Renewal Competence of Fetal Human Oligodendrocyte Progenitor Cells. *Journal of Neuroscience*, 32(43), 15066–15075. <https://doi.org/10.1523/JNEUROSCI.1320-12.2012>
- Miao, J., Ding, M., Zhang, A., Xiao, Z., Qi, W., Luo, N., Di, W., Tao, Y., & Fang, Y. (2012). Pleiotrophin promotes microglia proliferation and secretion of neurotrophic factors by activating extracellular signal-regulated kinase 1/2 pathway. *Neuroscience Research*, 74(3–4), 269–276. <https://doi.org/10.1016/j.neures.2012.09.001>
- Miao, J., Wang, F., Wang, R., Zeng, J., Zheng, C., & Zhuang, G. (2019). Pleiotrophin regulates functional heterogeneity of microglia cells in EAE animal models of multiple sclerosis by activating CCR-7/CD206 molecules and functional cytokines. *American Journal of Translational Research*, 11(4), 15.
- Momosaki, R., Yasunaga, H., Kakuda, W., Matsui, H., Fushimi, K., & Abo, M. (2016). Very Early versus Delayed Rehabilitation for Acute Ischemic Stroke Patients with Intravenous Recombinant Tissue Plasminogen Activator: A Nationwide Retrospective Cohort Study. *Cerebrovascular Diseases*, 42(1–2), 41–48. <https://doi.org/10.1159/000444720>

- Murphy, T. H., & Corbett, D. (2009). Plasticity during stroke recovery: From synapse to behaviour. *Nature Reviews Neuroscience*, *10*(12), 861–872.
<https://doi.org/10.1038/nrn2735>
- Muzzu, T., Mitolo, S., Gava, G. P., & Schultz, S. R. (2018). Encoding of locomotion kinematics in the mouse cerebellum. *PLOS ONE*, *13*(9), e0203900.
<https://doi.org/10.1371/journal.pone.0203900>
- Nakayama, H., Stig Jørgensen, H., Otto Raaschou, H., & Skyhøj Olsen, T. (1994). Recovery of upper extremity function in stroke patients: The Copenhagen stroke study. *Archives of Physical Medicine and Rehabilitation*, *75*(4), 394–398. [https://doi.org/10.1016/0003-9993\(94\)90161-9](https://doi.org/10.1016/0003-9993(94)90161-9)
- Ng, S.-C., de la Monte, S. M., Conboy, G. L., Karns, L. R., & Fishman, M. C. (1988). Cloning of Human GAP-43: Growth Association and Ischemic Resurgence. *Neuron*, *1*, 133–139.
- Nikolakopoulou, A. M., Montagne, A., Kisler, K., Dai, Z., Wang, Y., Huuskonen, M. T., Sagare, A. P., Lazic, D., Sweeney, M. D., Kong, P., Wang, M., Owens, N. C., Lawson, E. J., Xie, X., Zhao, Z., & Zlokovic, B. V. (2019). Pericyte loss leads to circulatory failure and pleiotrophin depletion causing neuron loss. *Nature Neuroscience*, *22*(7), 1089–1098.
<https://doi.org/10.1038/s41593-019-0434-z>
- Nudo, R. J. (2007). Postinfarct Cortical Plasticity and Behavioral Recovery. *Stroke*, *38*(2), 840–845. <https://doi.org/10.1161/01.STR.0000247943.12887.d2>
- Obembe, A. O., Simpson, L. A., Sakakibara, B. M., & Eng, J. J. (2019). Healthcare utilization after stroke in Canada- a population based study. *BMC Health Services Research*, *19*(1), 192. <https://doi.org/10.1186/s12913-019-4020-6>

- Obermeyer, J. M., Tuladhar, A., Payne, S. L., Ho, E., Morshead, C. M., & Shoichet, M. S. (2019). Local Delivery of Brain-Derived Neurotrophic Factor Enables Behavioral Recovery and Tissue Repair in Stroke-Injured Rats. *Tissue Engineering Part A*, 25(15–16), 1175–1187. <https://doi.org/10.1089/ten.tea.2018.0215>
- Ohab, J. J., Fleming, S., Blesch, A., & Carmichael, S. T. (2006). A Neurovascular Niche for Neurogenesis after Stroke. *Journal of Neuroscience*, 26(50), 13007–13016. <https://doi.org/10.1523/JNEUROSCI.4323-06.2006>
- Oshima, T., Lee, S., Sato, A., Oda, S., Hirasawa, H., & Yamashita, T. (2009). TNF- α contributes to axonal sprouting and functional recovery following traumatic brain injury. *Brain Research*, 1290, 102–110. <https://doi.org/10.1016/j.brainres.2009.07.022>
- Overman, J. J., & Carmichael, S. T. (2014). Plasticity in the Injured Brain: More than Molecules Matter. *The Neuroscientist*, 20(1), Article 1. <https://doi.org/10.1177/1073858413491146>
- Parish, C. L., Finkelstein, D. I., Tripanichkul, W., Satoskar, A. R., Drago, J., & Horne, M. K. (2002). The Role of Interleukin-1, Interleukin-6, and Glia in Inducing Growth of Neuronal Terminal Arbors in Mice. *The Journal of Neuroscience*, 22(18), 8034–8041. <https://doi.org/10.1523/JNEUROSCI.22-18-08034.2002>
- Patterson, S. L. (2015). Immune dysregulation and cognitive vulnerability in the aging brain: Interactions of microglia, IL-1 β , BDNF and synaptic plasticity. *Neuropharmacology*, 96, 11–18. <https://doi.org/10.1016/j.neuropharm.2014.12.020>
- Paveliev, M., Fenrich, K. K., Kislin, M., Kuja-Panula, J., Kuleskiy, E., Varjosalo, M., Kajander, T., Mugantseva, E., Ahonen-Bishopp, A., Khiroug, L., Kuleskaya, N., Rougon, G., & Rauvala, H. (2016). HB-GAM (pleiotrophin) reverses inhibition of neural regeneration

by the CNS extracellular matrix. *Scientific Reports*, 6(1).

<https://doi.org/10.1038/srep33916>

Peria, F. M., Neder, L., Marie, S. K. N., Rosemberg, S., Oba-Shinjo, S. M., Colli, B. O., Gabbai, A. A., Malheiros, S. M. F., Zago, M. A., Panepucci, R. A., Moreira-Filho, C. A., Okamoto, O. K., & Carlotti, C. G. (2007). Pleiotrophin expression in astrocytic and oligodendroglial tumors and it's correlation with histological diagnosis, microvascular density, cellular proliferation and overall survival. *Journal of Neuro-Oncology*, 84(3), 255–261. <https://doi.org/10.1007/s11060-007-9379-2>

Pomeroy, V. M., Cloud, G., Tallis, R. C., Donaldson, C., Nayak, V., & Miller, S. (2007). Transcranial Magnetic Stimulation and Muscle Contraction to Enhance Stroke Recovery: A Randomized Proof-of-Principle and Feasibility Investigation. *Neurorehabilitation and Neural Repair*, 21(6), 509–517. <https://doi.org/10.1177/1545968307300418>

Rauvala, H., Vanhala, A., Castre'n, E., Nolo, R., Raulo, E., Merenmies, J., & Panula, P. (1994). Expression of HB-GAM (heparin-binding growth-associated molecules) in the pathways of developing axonal processes in vivo and neurite outgrowth in vitro induced by HB-GAM. *Developmental Brain Research*, 79(2), 157–176. [https://doi.org/10.1016/0165-3806\(94\)90121-X](https://doi.org/10.1016/0165-3806(94)90121-X)

Reyes-Mata, M. P., Rojas-Mayorquín, A. E., Carrera-Quintanar, L., González-Castillo, C., Mireles-Ramírez, M. A., Guerrero-García, J. de J., & Ortuño-Sahagún, D. (2021). Pleiotrophin serum level is increased in Relapsing-Remitting Multiple Sclerosis and correlates with sex, BMI and treatment. *Archives of Medical Research*, S0188440921001405. <https://doi.org/10.1016/j.arcmed.2021.06.005>

- Risedal, A., Zeng, Rj., & Johansson, B. B. (1999). Early Training May Exacerbate Brain Damage after Focal Brain Ischemia in the Rat. *Journal of Cerebral Blood Flow & Metabolism*, *19*(9), 997–1003. <https://doi.org/10.1097/00004647-199909000-00007>
- Ross, A. M., Hurn, P., Perrin, N., Wood, L., Carlini, W., & Potempa, K. (2007). Evidence of the Peripheral Inflammatory Response in Patients With Transient Ischemic Attack. *Journal of Stroke and Cerebrovascular Diseases*, *16*(5), Article 5. <https://doi.org/10.1016/j.jstrokecerebrovasdis.2007.05.002>
- Rothman, S. M., & Olney, J. W. (1986). Glutamate and the pathophysiology of hypoxic–ischemic brain damage. *Annals of Neurology*, *19*(2), 105–111. <https://doi.org/10.1002/ana.410190202>
- Saito, A. (2004). Neuroprotective Role of a Proline-Rich Akt Substrate in Apoptotic Neuronal Cell Death after Stroke: Relationships with Nerve Growth Factor. *Journal of Neuroscience*, *24*(7), 1584–1593. <https://doi.org/10.1523/JNEUROSCI.5209-03.2004>
- Saleem, A. B., Ayaz, A., Jeffery, K. J., Harris, K. D., & Carandini, M. (2013). Integration of visual motion and locomotion in mouse visual cortex. *Nature Neuroscience*, *16*(12), 1864–1869. <https://doi.org/10.1038/nn.3567>
- Saleh, A., Smith, D. R., Balakrishnan, S., Dunn, L., Martens, C., Tweed, C. W., & Fernyhough, P. (2011). Tumor necrosis factor- α elevates neurite outgrowth through an NF- κ B-dependent pathway in cultured adult sensory neurons: Diminished expression in diabetes may contribute to sensory neuropathy. *Brain Research*, *1423*, 87–95. <https://doi.org/10.1016/j.brainres.2011.09.029>

- Sandrini, M., & Cohen, L. G. (2013). Noninvasive brain stimulation in neurorehabilitation. In *Handbook of Clinical Neurology* (Vol. 116, pp. 499–524). Elsevier.
<https://doi.org/10.1016/B978-0-444-53497-2.00040-1>
- Schaar, K. L., Brenneman, M. M., & Savitz, S. I. (2010). Functional assessments in the rodent stroke model. *Experimental & Translational Stroke Medicine*, 2(1), 13.
<https://doi.org/10.1186/2040-7378-2-13>
- Schain, A. J., Hill, R. A., & Grutzendler, J. (2014). Label-free in vivo imaging of myelinated axons in health and disease with spectral confocal reflectance microscopy. *Nature Medicine*, 20(4), 443–449. <https://doi.org/10.1038/nm.3495>
- Scolding, N. J., Frith, S., Linington, C., Morgan, B. P., Campbell, A. K., & Compston, D. A. S. (1989). Myelin-oligodendrocyte glycoprotein (MOG) is a surface marker of oligodendrocyte maturation. *Journal of Neuroimmunology*, 22(3), 169–176.
[https://doi.org/10.1016/0165-5728\(89\)90014-3](https://doi.org/10.1016/0165-5728(89)90014-3)
- Shanina, E. V., Schallert, T., Witte, O. W., & Redeker, C. (2006). Behavioral recovery from unilateral photothrombotic infarcts of the forelimb sensorimotor cortex in rats: Role of the contralateral cortex. *Neuroscience*, 139(4), 1495–1506.
<https://doi.org/10.1016/j.neuroscience.2006.01.016>
- Silver, J., & Miller, J. H. (2004). Regeneration beyond the glial scar. *Nature Reviews Neuroscience*, 5(2), 146–156. <https://doi.org/10.1038/nrn1326>
- Sims, N. R., & Yew, W. P. (2017). Reactive astrogliosis in stroke: Contributions of astrocytes to recovery of neurological function. *Neurochemistry International*, 107, 88–103.
<https://doi.org/10.1016/j.neuint.2016.12.016>

- Sims, S.-K., Wilken-Resman, B., Smith, C. J., Mitchell, A., McGonegal, L., & Sims-Robinson, C. (2022). Brain-Derived Neurotrophic Factor and Nerve Growth Factor Therapeutics for Brain Injury: The Current Translational Challenges in Preclinical and Clinical Research. *Neural Plasticity*, 2022, 1–15. <https://doi.org/10.1155/2022/3889300>
- Sist, B., Fouad, K., & Winship, I. R. (2014). Plasticity beyond peri-infarct cortex: Spinal up regulation of structural plasticity, neurotrophins, and inflammatory cytokines during recovery from cortical stroke. *Experimental Neurology*, 252, 47–56. <https://doi.org/10.1016/j.expneurol.2013.11.019>
- Smith, M.-C., Byblow, W. D., Barber, P. A., & Stinear, C. M. (2017). Proportional Recovery From Lower Limb Motor Impairment After Stroke. *Stroke*, 48(5), 1400–1403. <https://doi.org/10.1161/STROKEAHA.116.016478>
- Smith, W. S., Sung, G., Saver, J., Budzik, R., Duckwiler, G., Liebeskind, D. S., Lutsep, H. L., Rymer, M. M., Higashida, R. T., Starkman, S., & Gobin, Y. P. (2008). Mechanical Thrombectomy for Acute Ischemic Stroke: Final Results of the Multi MERCI Trial. *Stroke*, 39(4), 1205–1212. <https://doi.org/10.1161/STROKEAHA.107.497115>
- Soleman, S., Yip, P. K., Duricki, D. A., & Moon, L. D. F. (2012). Delayed treatment with chondroitinase ABC promotes sensorimotor recovery and plasticity after stroke in aged rats. *Brain*, 135(4), Article 4. <https://doi.org/10.1093/brain/aws027>
- Stroemer, R. P., Kent, T. A., & Hulsebosch, C. E. (1993). Acute increase in expression of growth associated protein GAP-43 following cortical ischemia in rat. *Neuroscience Letters*, 162(1–2), 51–54. [https://doi.org/10.1016/0304-3940\(93\)90557-2](https://doi.org/10.1016/0304-3940(93)90557-2)

- Stroemer, R. P., Kent, T. A., & Hulsebosch, C. E. (1995). Neocortical Neural Sprouting, Synptogenesis, and Behavioral Recovery After Neocortical Infarction in Rats. *Stroke*, 26(11), Article 11. <https://doi.org/10.1161/01.STR.26.11.2135>
- Suzuki, S., Tanaka, K., & Suzuki, N. (2009). Ambivalent Aspects of Interleukin-6 in Cerebral Ischemia: Inflammatory versus Neurotrophic Aspects. *Journal of Cerebral Blood Flow & Metabolism*, 29(3), 464–479. <https://doi.org/10.1038/jcbfm.2008.141>
- Szaflarski, J. P., Page, S. J., Kissela, B. M., Lee, J.-H., Levine, P., & Strakowski, S. M. (2006). Cortical Reorganization Following Modified Constraint-Induced Movement Therapy: A Study of 4 Patients With Chronic Stroke. *Archives of Physical Medicine and Rehabilitation*, 87(8), 1052–1058. <https://doi.org/10.1016/j.apmr.2006.04.018>
- Takeuchi, N., & Izumi, S.-I. (2015). Combinations of stroke neurorehabilitation to facilitate motor recovery: Perspectives on Hebbian plasticity and homeostatic metaplasticity. *Frontiers in Human Neuroscience*, 9. <https://doi.org/10.3389/fnhum.2015.00349>
- Tang, Y., Li, M.-Y., Zhang, X., Jin, X., Liu, J., & Wei, P.-H. (2019). Delayed exposure to environmental enrichment improves functional outcome after stroke. *Journal of Pharmacological Sciences*, 140(2), 137–143. <https://doi.org/10.1016/j.jphs.2019.05.002>
- Tanga, N., Kuboyama, K., Kishimoto, A., Kiyonari, H., Shiraishi, A., Suzuki, R., Watanabe, T., Fujikawa, A., & Noda, M. (2019). The PTN-PTPRZ signal activates the AFAP1L2-dependent PI3K-AKT pathway for oligodendrocyte differentiation: Targeted inactivation of PTPRZ activity in mice. *Glia*, 67(5), 967–984. <https://doi.org/10.1002/glia.23583>
- Taravini, I. R., Chertoff, M., Cafferata, E. G., Courty, J., Murer, M. G., Pitossi, F. J., & Gershanik, O. S. (2011). Pleiotrophin over-expression provides trophic support to

- dopaminergic neurons in parkinsonian rats. *Molecular Neurodegeneration*, 6(1), 40.
<https://doi.org/10.1186/1750-1326-6-40>
- Tennant, K. A., Adkins, D. L., Donlan, N. A., Asay, A. L., Thomas, N., Kleim, J. A., & Jones, T. A. (2011). The Organization of the Forelimb Representation of the C57BL/6 Mouse Motor Cortex as Defined by Intracortical Microstimulation and Cytoarchitecture. *Cerebral Cortex*, 21(4), 865–876. <https://doi.org/10.1093/cercor/bhq159>
- Tonchev, A. B. (2011). Brain ischemia, neurogenesis, and neurotrophic receptor expression in primates. *Archives Italiennes De Biologie*, 149(2), Article 2.
<https://doi.org/10.4449/aib.v149i2.1368>
- Uzdensky, A. B. (2018). Photothrombotic Stroke as a Model of Ischemic Stroke. *Translational Stroke Research*, 9(5), 437–451. <https://doi.org/10.1007/s12975-017-0593-8>
- Uzdensky, A. B. (2019). Apoptosis regulation in the penumbra after ischemic stroke: Expression of pro- and antiapoptotic proteins. *Apoptosis*, 24(9–10), 687–702.
<https://doi.org/10.1007/s10495-019-01556-6>
- Wade, D. T., Langton-Hewer, R., Wood, V. A., Skilbeck, C. E., & Ismail, H. M. (1983). The hemiplegic arm after stroke: Measurement and recovery. *Journal of Neurology, Neurosurgery & Psychiatry*, 46(6), 521–524. <https://doi.org/10.1136/jnnp.46.6.521>
- Wanaka, A., Carroll, S. L., & Milbrandt, J. (1993). Developmentally regulated expression of pleiotrophin, a novel heparin binding growth factor, in the nervous system of the rat. *Developmental Brain Research*, 72(1), Article 1. [https://doi.org/10.1016/0165-3806\(93\)90166-8](https://doi.org/10.1016/0165-3806(93)90166-8)

- Wang, Y., Liu, G., Hong, D., Chen, F., Ji, X., & Cao, G. (2016). White matter injury in ischemic stroke. *Progress in Neurobiology, 141*, 45–60.
<https://doi.org/10.1016/j.pneurobio.2016.04.005>
- Wenner, P. (2011). Mechanisms of GABAergic Homeostatic Plasticity. *Neural Plasticity, 2011*, 1–6. <https://doi.org/10.1155/2011/489470>
- Wieloch, T., & Nikolich, K. (2006). Mechanisms of neural plasticity following brain injury. *Current Opinion in Neurobiology, 16*(3), 258–264.
<https://doi.org/10.1016/j.conb.2006.05.011>
- Wiersma, A. M., Fouad, K., & Winship, I. R. (2017). Enhancing Spinal Plasticity Amplifies the Benefits of Rehabilitative Training and Improves Recovery from Stroke. *The Journal of Neuroscience, 37*(45), 10983–10997. <https://doi.org/10.1523/JNEUROSCI.0770-17.2017>
- Wilson, H. C., Scolding, N. J., & Raine, C. S. (2006). Co-expression of PDGF α receptor and NG2 by oligodendrocyte precursors in human CNS and multiple sclerosis lesions. *Journal of Neuroimmunology, 176*(1–2), 162–173.
<https://doi.org/10.1016/j.jneuroim.2006.04.014>
- Winship, I. R., & Murphy, T. H. (2009). Remapping the Somatosensory Cortex after Stroke: Insight from Imaging the Synapse to Network. *The Neuroscientist, 15*(5), 507–524.
<https://doi.org/10.1177/1073858409333076>
- Wolf, S. L., Winstein, C. J., Miller, J. P., Taub, E., Uswatte, G., Morris, D., Giuliani, C., Light, K. E., Nichols-Larsen, D., & EXCITE Investigators, for the. (2006). Effect of Constraint-Induced Movement Therapy on Upper Extremity Function 3 to 9 Months After Stroke: The EXCITE Randomized Clinical Trial. *JAMA, 296*(17), Article 17.
<https://doi.org/10.1001/jama.296.17.2095>

- Xing, C., Arai, K., Lo, E. H., & Hommel, M. (2012). Pathophysiologic Cascades in Ischemic Stroke. *International Journal of Stroke*, 7(5), 378–385. <https://doi.org/10.1111/j.1747-4949.2012.00839.x>
- Xu, S., Lu, J., Shao, A., Zhang, J. H., & Zhang, J. (2020). Glial Cells: Role of the Immune Response in Ischemic Stroke. *Frontiers in Immunology*, 11. <https://doi.org/10.3389/fimmu.2020.00294>
- Yanagisawa, H., Komuta, Y., Kawano, H., Toyoda, M., & Sango, K. (2010). Pleiotrophin induces neurite outgrowth and up-regulates growth-associated protein (GAP)-43 mRNA through the ALK/GSK3 β / β -catenin signaling in developing mouse neurons. *Neuroscience Research*, 66(1), Article 1. <https://doi.org/10.1016/j.neures.2009.10.002>
- Yeh, H.-J., He, Y. Y., Xu, J., Hsu, C. Y., & Deuel, T. F. (1998). Upregulation of Pleiotrophin Gene Expression in Developing Microvasculature, Macrophages, and Astrocytes after Acute Ischemic Brain Injury. *The Journal of Neuroscience*, 18(10), 3699–3707. <https://doi.org/10.1523/JNEUROSCI.18-10-03699.1998>
- Yiu, G., & He, Z. (2006). Glial inhibition of CNS axon regeneration. *Nature Reviews Neuroscience*, 7(8), 617–627. <https://doi.org/10.1038/nrn1956>
- Zhao, C., Zhao, S., Guan, M., Cheng, X., Wang, H., Liu, C., Zhong, S., Zhou, Z., & Liang, Y. (2020). Forced forelimb use following stroke enhances oligodendrogenesis and functional recovery in the rat. *Brain Research*, 1746, 147016. <https://doi.org/10.1016/j.brainres.2020.147016>
- Zhao, S., Zhao, M., Xiao, T., Jolkkonen, J., & Zhao, C. (2013). Constraint-Induced Movement Therapy Overcomes the Intrinsic Axonal Growth–Inhibitory Signals in Stroke Rats. *Stroke*, 44(6), Article 6. <https://doi.org/10.1161/STROKEAHA.111.000361>

Zou, L. L., Huang, L., Hayes, R. L., Black, C., Qiu, Y. H., Perez-Polo, J. R., Le, W., Clifton, G. L., & Yang, K. (1999). Liposome-mediated NGF gene transfection following neuronal injury: Potential therapeutic applications. *Gene Therapy*, 6(6), 994–1005.
<https://doi.org/10.1038/sj.gt.3300936>

Appendix I: Figures

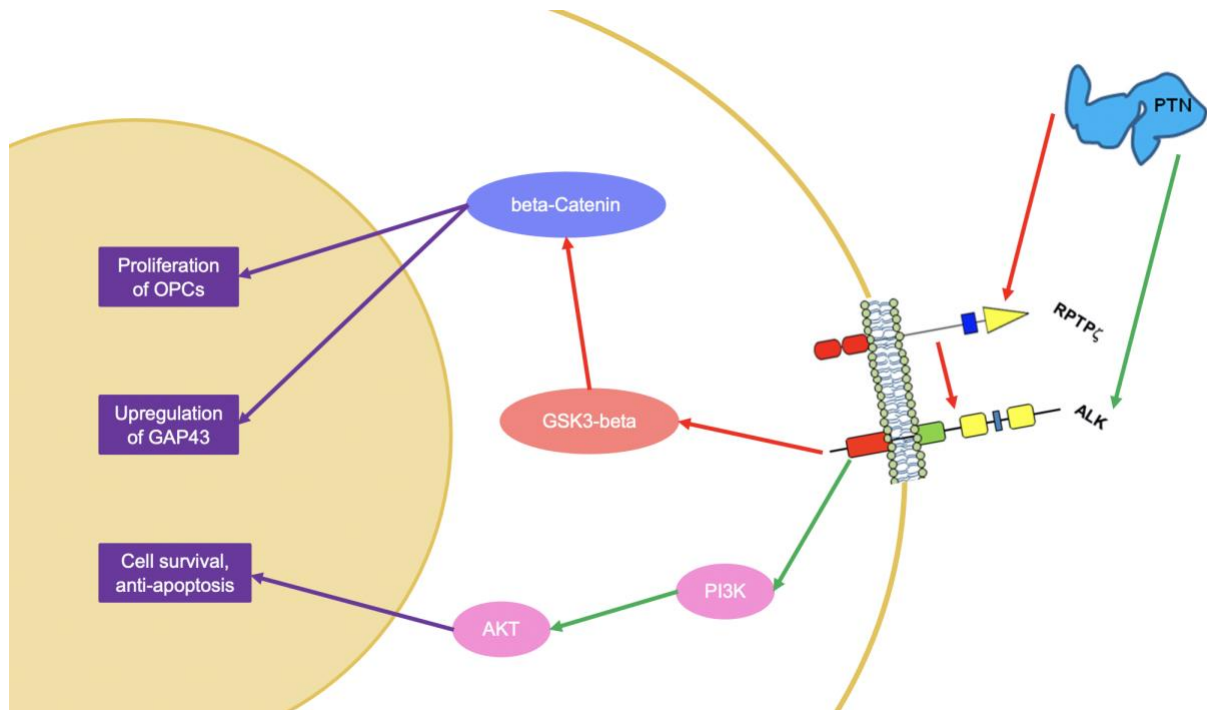


Figure 1. Diagram outlining pathways of interest that PTN acts on. PTN can activate ALK directly or indirectly, by inhibiting RPTP-beta/zeta which acts to dephosphorylate ALK. PTN activity therefore results in higher levels of phosphorylated ALK, which can activate 2 important pathways. Activated ALK can inhibit GSK3- β , which prevents the proteasomal degradation of beta-catenin. Accumulation of β -catenin contributes to the proliferation of OPCs and the upregulation of GAP43. Activated ALK also activates phosphoinositide 3-kinase (PI3K), which then phosphorylates AKT. Activated AKT promotes pathways of cell survival, anti-apoptosis, cell proliferation, and angiogenesis. One way it does this is through the activation of mechanistic target of rapamycin (mTOR).

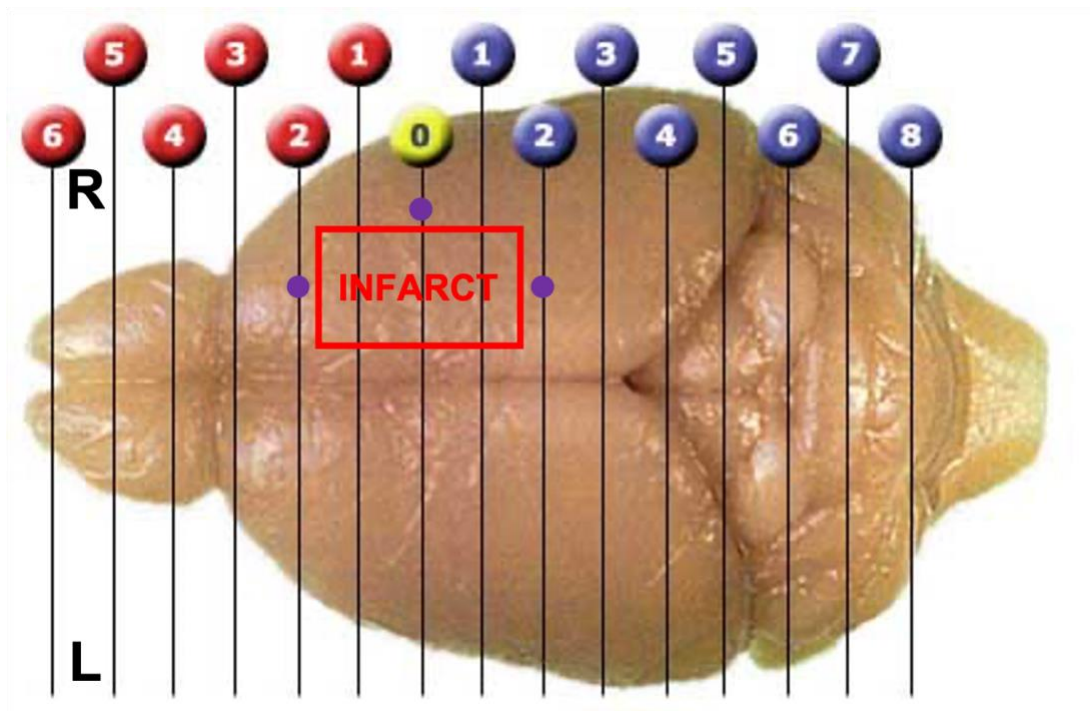


Figure 2. *Coordinates of infarct area and injection sites.* L indicates the left side of the brain and R indicates the right side of the brain for the purposes of orientation. The red box indicates the area that will be thinned and illuminated to induce photothrombotic stroke. The purple dots indicate the injection sites for cortical microinjection of PTN or its vehicle, PBS.

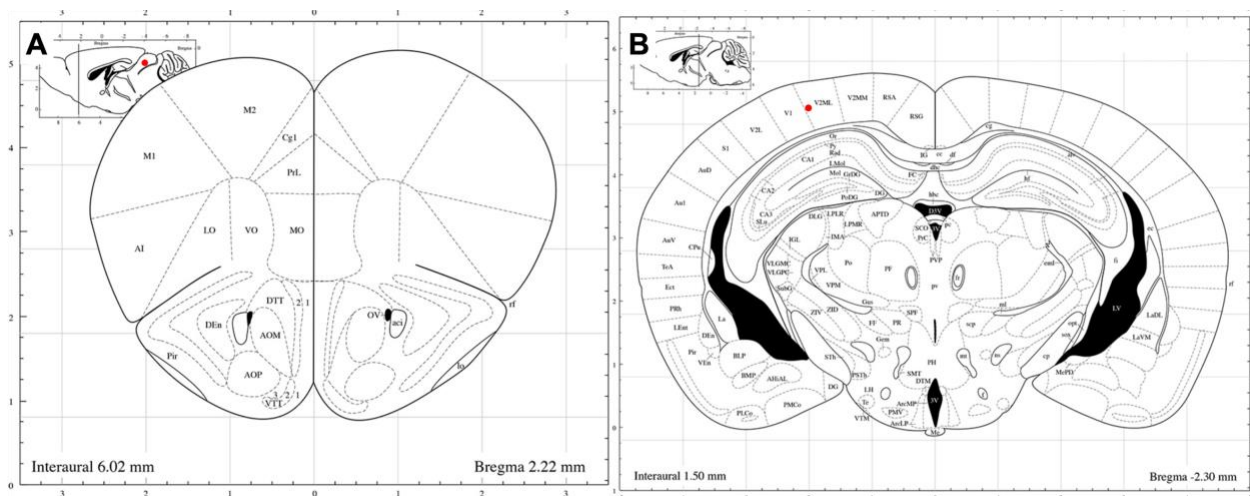


Figure 3. Start and end points of tissue collection. A) indicates the start point of tissue collection while sectioning and B) indicates the end point. This protocol spans 4800 microns of brain tissue rostro-caudally.

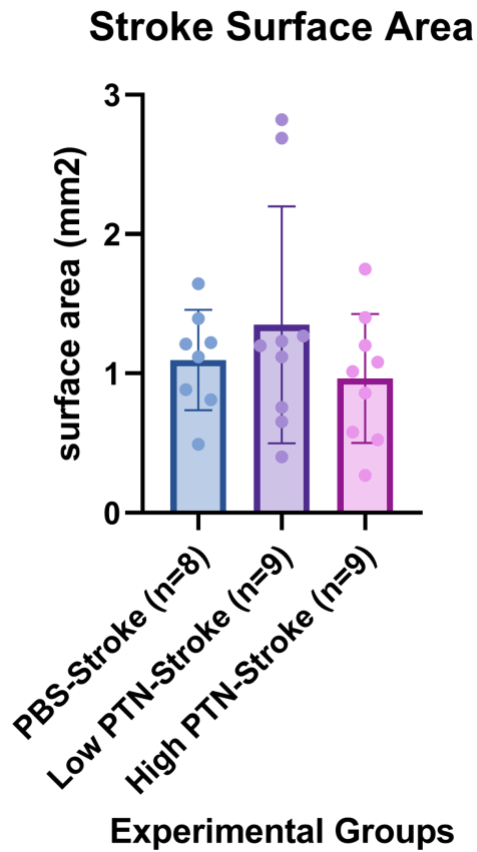


Figure 4. *Surface area of visible infarct on formalin-perfused brains.* Indicates the mean surface area in each stroke group, with individual values present and error bars displaying standard deviation (PBS-Stroke Mean=1.10 mm², SD=0.361 mm²; Low PTN-Stroke Mean=1.35 mm², SD=0.851 mm²; High PTN-Stroke Mean=0.964 mm², SD=0.463 mm²). The ROUT method for detecting outliers found one outlier in the PBS-Stroke group, which was removed prior to carrying out the Shapiro-Wilk test for normality and the consequent Kruskal-Wallis test for main effects. With an approximate P=0.631, no main effect of treatment on stroke surface area was observed.

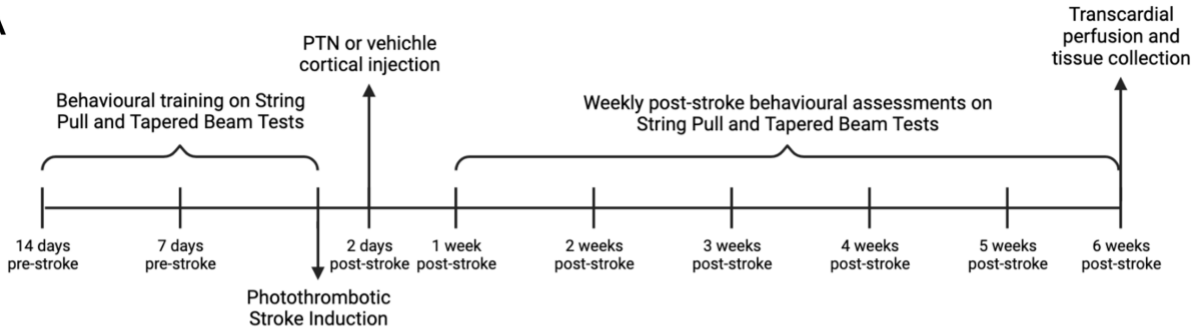
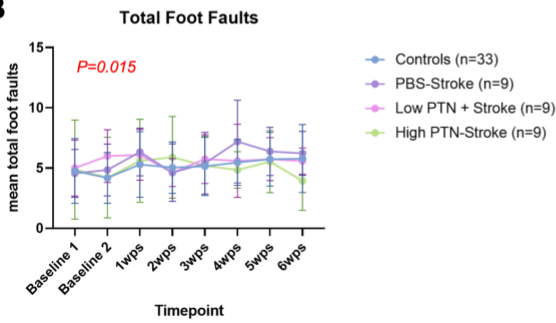
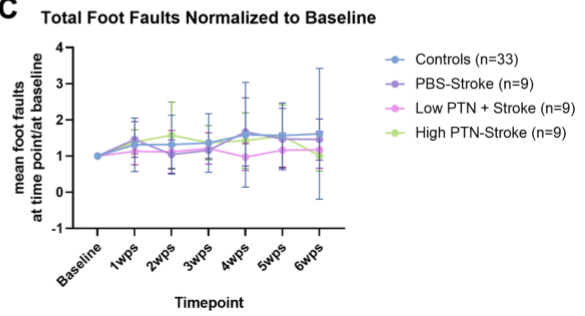
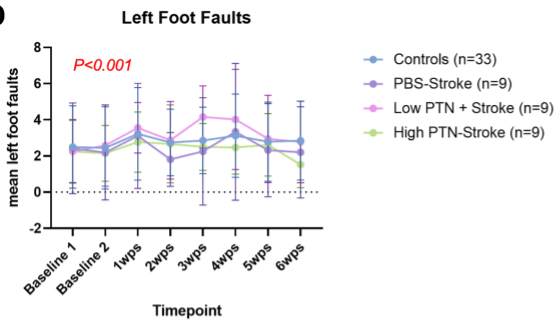
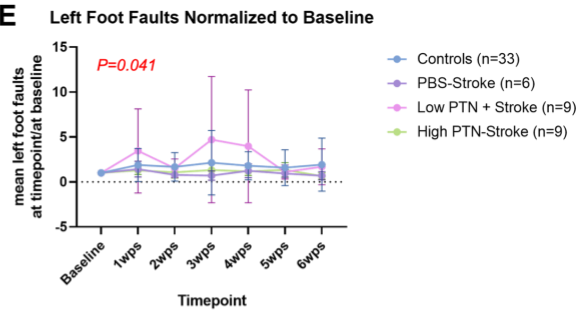
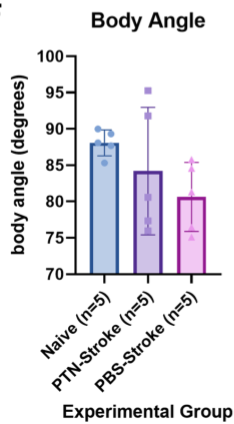
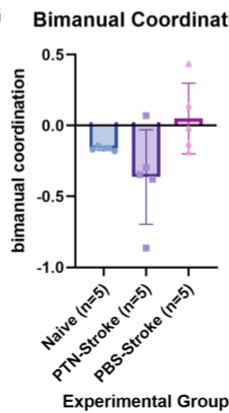
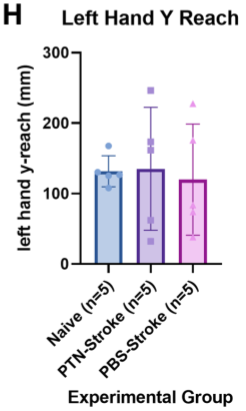
A**B****C****D****E****F****G****H**

Figure 5. *Behavioural outcomes following injury and treatment, assessed by the Tapered Beam and String Pull Tasks.* The abbreviation “wps” indicates “weeks post-stroke.” A) details the experimental timeline. B-E) displays results on the Tapered Beam task, with the control groups (Naive, PBS-Sham, Low PTN-Sham, and High PTN-Sham) pooled together. Error bars display the standard deviation. B) shows the mean total foot faults made per timepoint in each experimental group. Though two-way ANOVA revealed a main effect of time ($P=0.015$), Šídák’s multiple comparisons test did not reveal any significance between timepoints within any treatment group. C) shows the mean total foot faults made per timepoint in each experimental group, normalized to baseline. Two-way ANOVA revealed no main effects in this measure. D) shows mean left foot faults made per timepoint in each experimental group. Though two-way ANOVA revealed a main effect of time ($P<0.001$), Šídák’s multiple comparisons test did not reveal any significance between timepoints within any treatment group. E) shows mean left foot faults made per timepoint in each experimental group, normalized to baseline. Two-way ANOVA revealed a main effect of time ($P=0.041$), though Šídák’s multiple comparisons test did not reveal a significant difference between any timepoint within treatment groups. 3 animals were excluded from the PBS-Stroke group in this measurement due to their baseline measure of left foot faults being equal to 0. F-H) displays results on the String Pull task at 1 week post-stroke for animals selected while researcher remained blinded. The animals in the PTN-Stroke group received the 5 mg/ml dosage of PTN. F) shows body angle in each experimental group at 1 week post-stroke, where Kruskal-Wallis test revealed no main effect ($P=0.145$). Naive Mean= 88.1° , SD= 1.80° ; PTN-Stroke Mean= 84.2° , SD= 8.78° ; PBS-Stroke Mean= 80.6° , SD= 4.74° . G) shows bimanual coordination in each experimental group at 1 week post-stroke, where ordinary one-way ANOVA (*cont. overleaf*) revealed no main effect ($P=0.056$). Naive Mean= -0.162 , SD= 0.0130 ; PTN-Stroke Mean= -0.363 ,

SD=0.333; PBS-Stroke Mean=0.0501, SD=0.249. H) shows the Y-reach of the left hand, or the vertical distance travelled by the left hand during reach motion, at 1 week posts-stroke, where ordinary one-way ANOVA revealed no main effect ($P=0.935$). Naive Mean=132 mm, SD=21.9 mm; PTN-Stroke Mean=135 mm, SD=87.2 mm; PBS-Stroke Mean=120 mm, SD=78.8 mm).

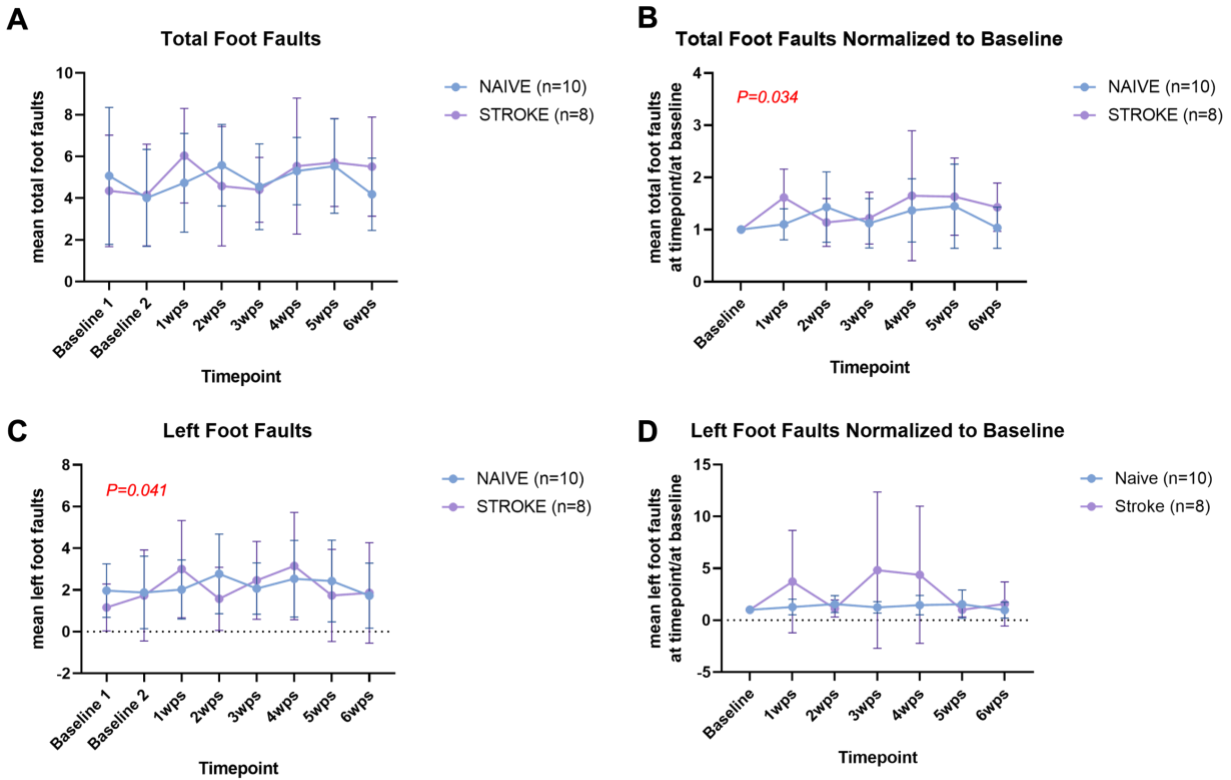


Figure 6. Tapered Beam performance when selecting for the largest observed strokes. The abbreviation “wps” indicates “weeks post-stroke.” The 8 animals with the largest strokes were selected, regardless of treatment, and pooled together as a Stroke group to compare to Naive animals. The error bars show standard deviation. A) shows mean total foot faults made by each group at each timepoint. Two-way ANOVA revealed no main effects. When total foot fault measures were normalized to baseline (B) two-way ANOVA revealed a main effect of time ($P=0.034$), but no significant comparisons between timepoints within treatment groups were observed. C) shows mean left foot faults made by each group at each timepoint. Two-way ANOVA revealed a main effect of time ($P=0.041$), but no significant comparisons were observed between timepoints within treatment groups. When left foot faults were normalized to baseline (D) two-way ANOVA revealed no main effects.

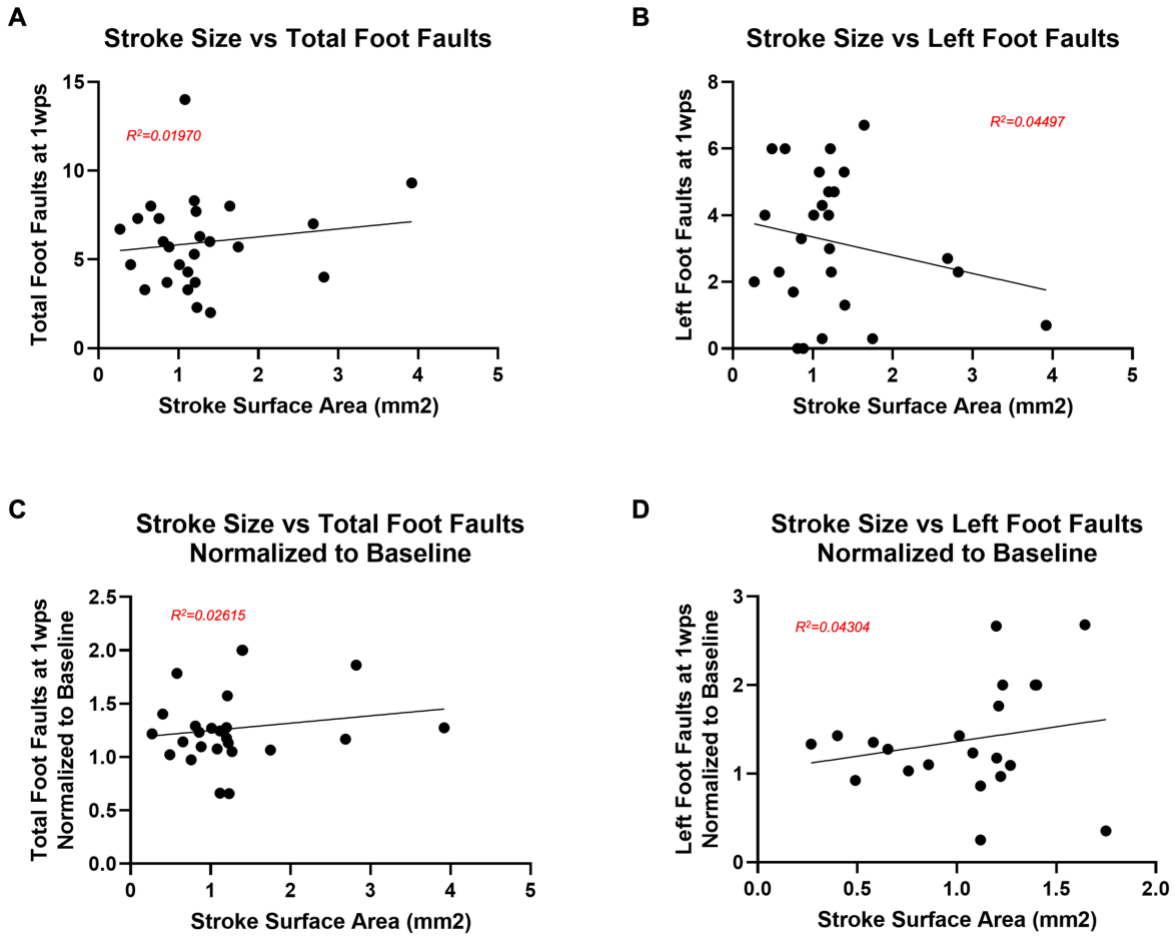


Figure 7. Correlation between stroke surface area and performance on Tapered Beam task measures (caption overleaf).

Figure 7. The abbreviation “wps” indicates “weeks post-stroke.” Performance on selected measures of Tapered Beam were plotted against the calculated stroke surface area for animals in all stroke groups. A) shows total foot faults at 1 week post-stroke plotted against stroke surface area at 6 weeks post-stroke (n=26). No significant correlation was found (P=0.4941). B) shows left foot faults at 1 week post stroke plotted against stroke surface at 6 weeks post-stroke (n=26). No significant correlation was found (P=0.2983). C) shows total foot faults at 1 week post-stroke normalized to baseline plotted against stroke surface area at 6 weeks post-stroke (n=25). 1 animal was detected as an outlier and excluded. No significant correlation was found (P=0.1254). D) shows left foot faults at 1 week post-stroke normalized to baseline plotted against stroke surface area at 6 weeks post-stroke (n=21). 2 animals were excluded due to being outliers and 3 animals were excluded due to the baseline measurement of left foot faults being equal to zero (normalization not possible). No significant correlation was found (P=0.3669).

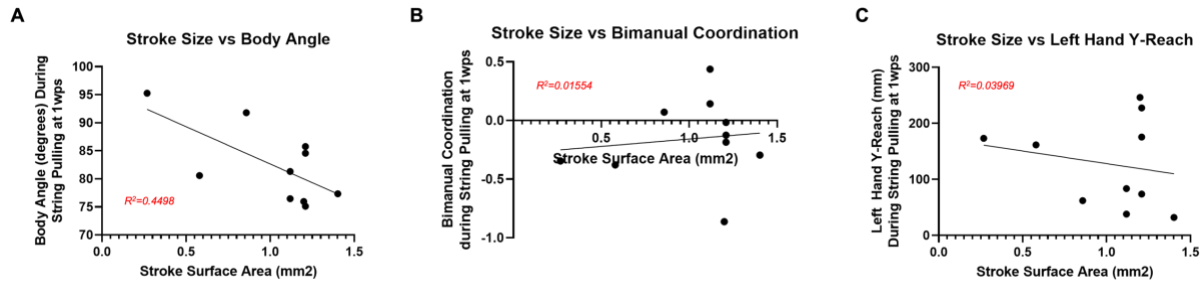


Figure 8. *Correlation between stroke surface area and performance on String Pull task measures.*

The abbreviation “wps” indicates “weeks post-stroke.” Performance on selected measures of String Pull were plotted against the calculated stroke surface area for the animals in PBS-Stroke and PTN-Stroke groups (n=10). A) shows body angle during string pulling motion at 1 week post-stroke plotted against stroke surface area at 6 weeks post-stroke. A significant correlation was observed between these measures (P=0.0338). B) shows bimanual coordination during string pulling motion at 1 week post-stroke plotted against stroke surface area at 6 weeks post-stroke. No significant correlation was observed between these measures (P=0.7315). C) shows the vertical distance travelled by the left hand during reaching (Y-reach of the left hand) at 1 week post-stroke plotted against stroke surface area at 6 weeks post-stroke. No significant correlation was observed between these measures (P=0.5811).

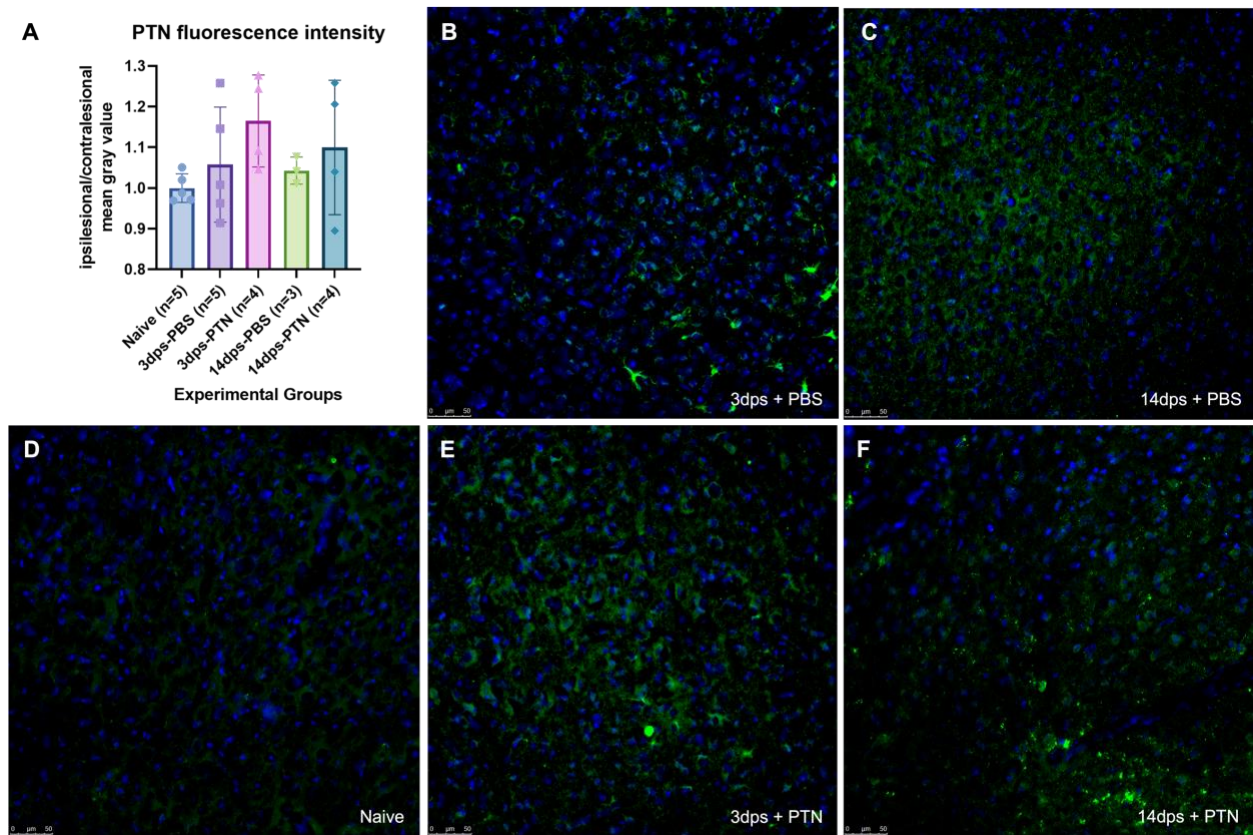


Figure 9. Mean fluorescence intensity of PTN immunohistochemistry at 3 days and 14 days post-stroke. The abbreviation “dps” indicates “days post-stroke.” A) Mean fluorescence intensity of PTN in each experimental group with error bars showing standard deviation (Naive Mean=1.00, SD=0.0350; 3dps-PBS Mean=1.06, SD=0.141; 3dps-PTN Mean=1.16, SD=0.113; 14dps-PBS Mean=1.04, SD=0.0332; 14dps-PTN Mean=1.10, SD=0.165). Ordinary one-way ANOVA revealed no main effect ($P=0.313$). B-F) show representative images from each experimental group, detailed in the bottom right corner of each image. PTN is shown in green and DAPI is shown in blue.

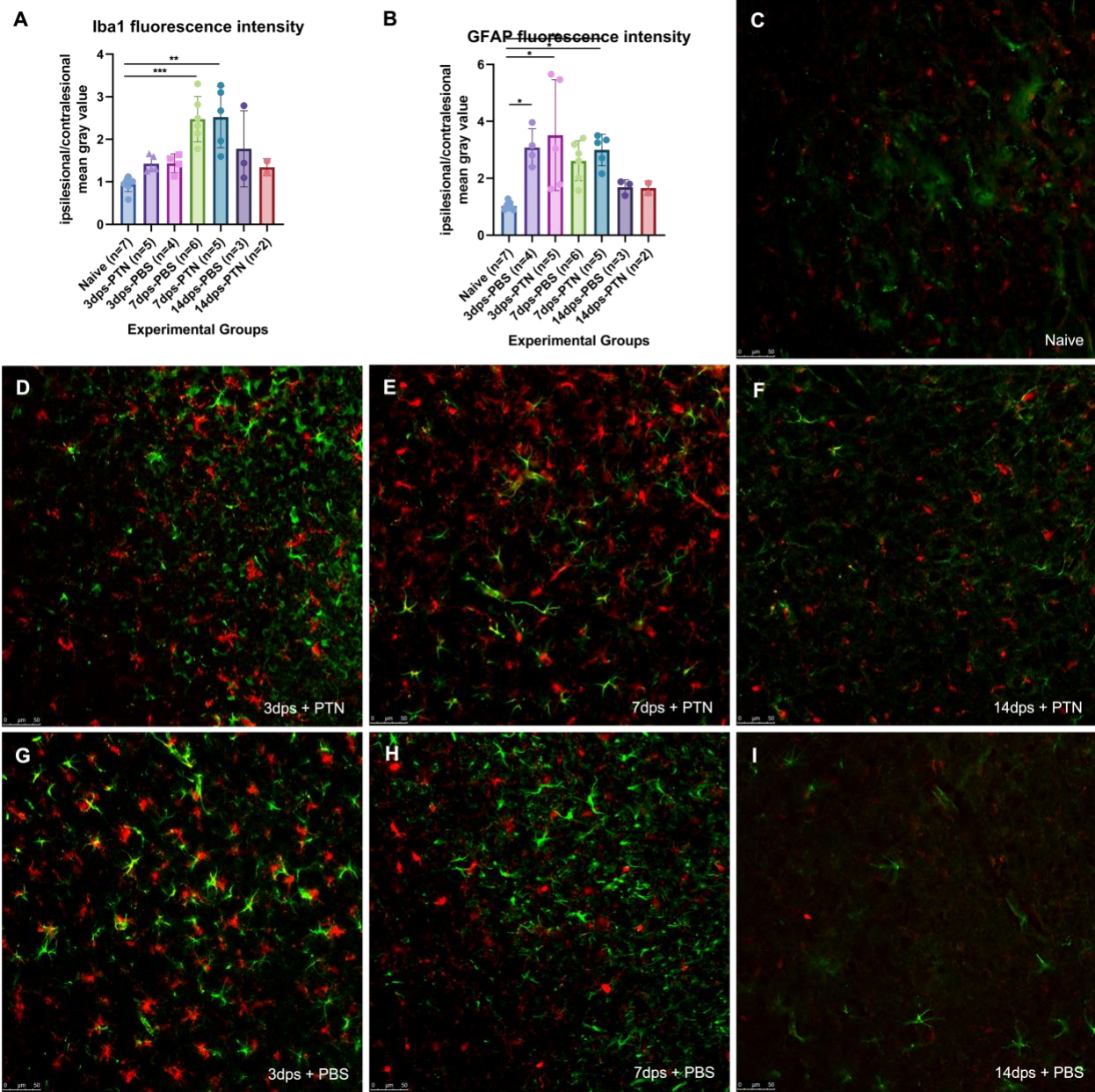


Figure 10. Mean fluorescence intensity of Iba1 and GFAP to indicate reactivity of microglia and astrocytes, respectively, from 3 to 14 days post-stroke (caption overleaf).

Figure 10. The abbreviation “dps” indicates “days post-stroke.” A) Mean fluorescence intensity of Iba1 in each experimental group with error bars showing standard deviation (Naive Mean=0.946, SD=0.173; 3dps-PTN Mean=1.43, SD=0.224; 3dps-PBS Mean=1.43, SD=0.187; 7dps-PBS Mean=2.48, SD=0.535; 7dps-PTN Mean=2.52, SD=0.722; 14dps-PBS Mean=1.78, SD=0.895; 14dps-PTN Mean=1.35, SD=0.200). Kruskal-Wallis test revealed a main effect ($P<0.001$). Dunn’s multiple comparisons test showed a significant difference between Naive and 7dps-PBS groups (marked as *** above, $p<0.001$) and Naive and 7dps-PTN groups (marked as ** above, $p=0.001$). B) Mean fluorescence intensity of GFAP in each experimental group with error bars showing standard deviation (Naive Mean=1.03, SD=0.138; 3dps-PBS Mean=3.08, SD=0.662; 3dps-PTN Mean=3.51, SD=1.95; 7dps-PBS Mean=2.61, SD=0.703; 7dps-PTN Mean=3.00, SD=0.553; 14dps-PBS Mean=1.69, SD=0.260; 14dps-PTN Mean=1.66, SD=0.249). Kruskal-Wallis test revealed a main effect ($P=0.002$). Dunn’s multiple comparisons test showed a significant difference between Naive and 3dps-PBS groups (marked as * above, $p=0.022$), Naive and 3dps-PTN groups (marked as * above, $p=0.025$), Naive and 7dps-PBS groups (marked as * above, $p=0.046$), and Naive and 7dps-PTN groups (marked as ** above, $p=0.007$). C-I) show representative images from each experimental group, detailed in the bottom right corner of each image. Iba1 is shown in red and GFAP is shown in green.

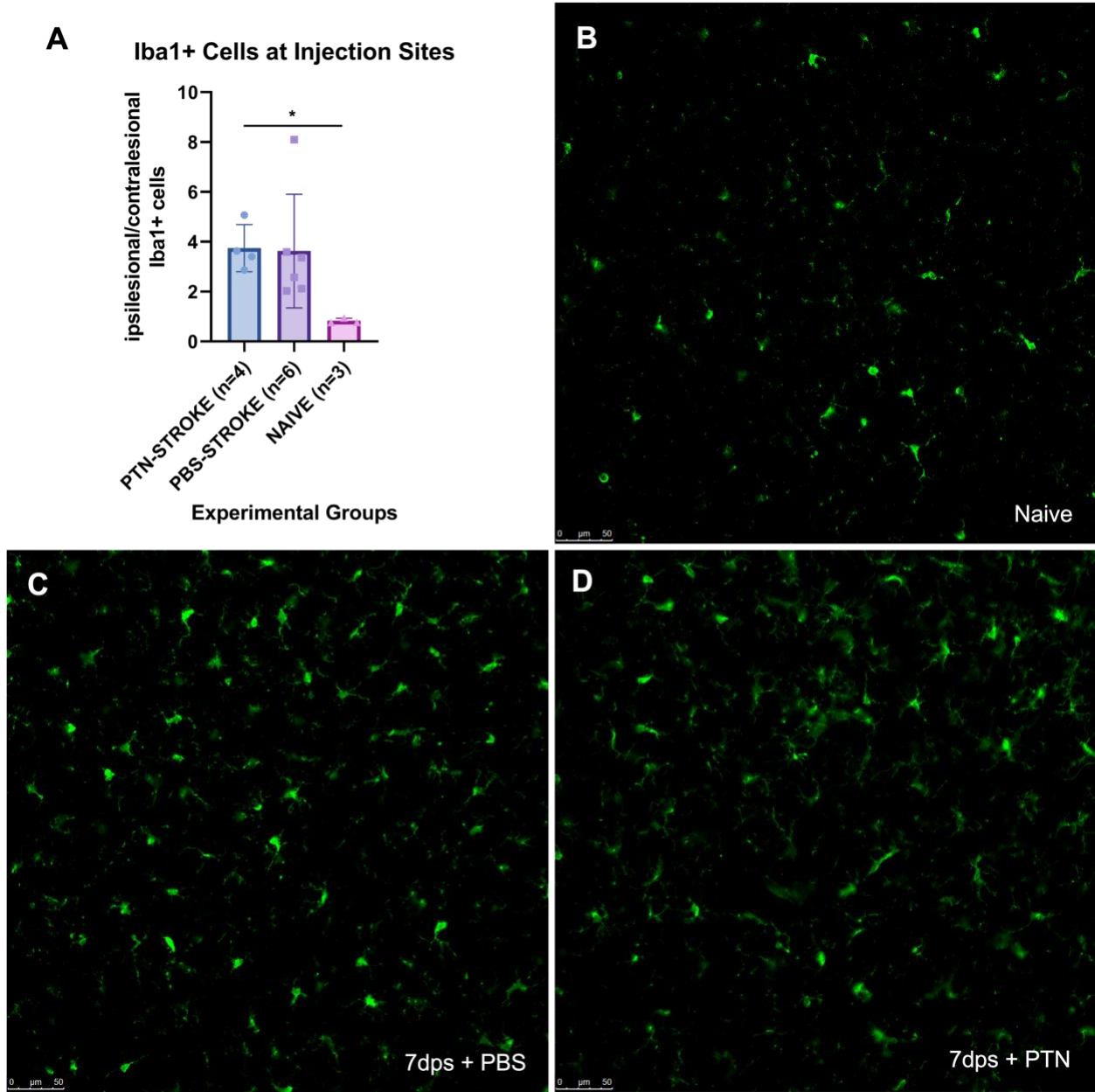


Figure 11. *Iba1*+ cells counted in the ipsilesional cortex normalized to *Iba1*+ cell count in the contralesional cortex at 7 days post-stroke (caption overleaf).

Figure 11. The abbreviation “dps” indicates “days post-stroke.” A) Mean Iba1+ cells in the ipsilesional cortex normalized to Iba1+ cell count in the contralesional cortex with error bars indicating standard deviation (PTN-STROKE Mean=3.743, SD=0.9440; PBS-STROKE Mean=3.628, SD=2.280; NAIVE Mean=0.8267, SD=0.1021). Kruskal-Wallis test revealed a main effect (P=0.0141). Dunn’s multiple comparisons test revealed a significant difference in ipsilesional/contralesional Iba+ cells between PTN-STROKE animals and NAIVE animals (marked as * above, p=0.0275). C-D) show representative images from each experimental group, which is detailed in the bottom right corner. Iba1 is shown in green.

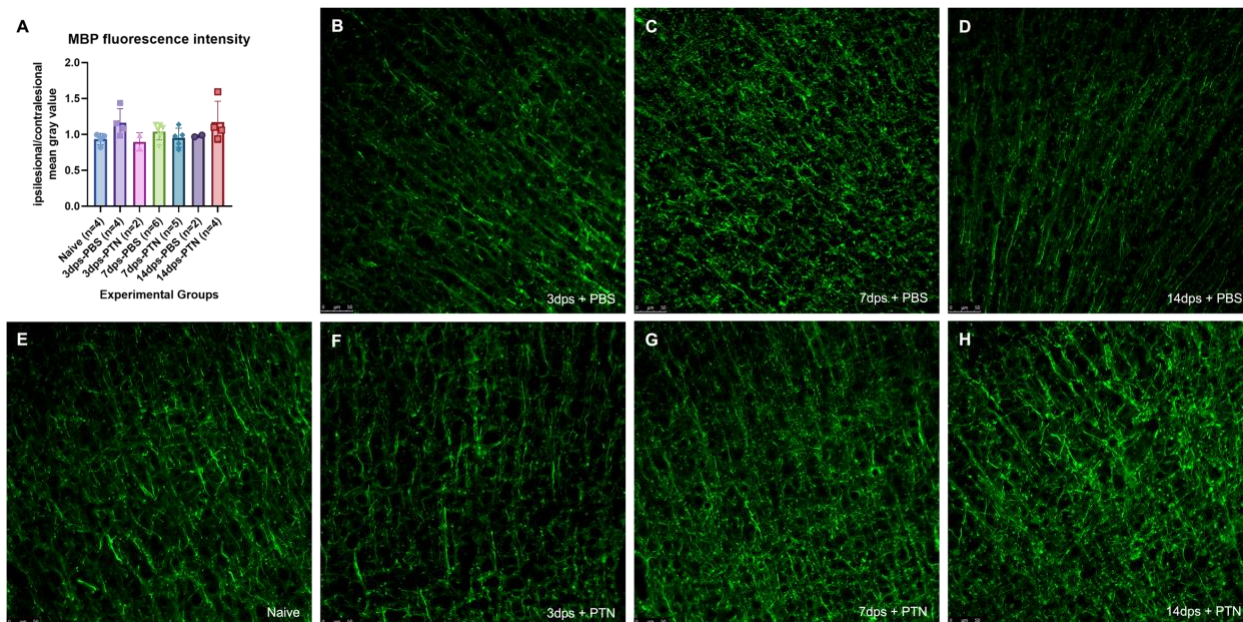


Figure 12. Mean fluorescence intensity of MBP to indicate presence of myelin from 3 to 14 days post-stroke. The abbreviation “dps” indicates “days post-stroke.” A) Mean fluorescence intensity in each experimental group with error bars showing standard deviation (Naive Mean=0.935, SD=0.0795; 3dps-PBS Mean=1.16, SD=0.195; 3dps-PTN Mean=0.897, SD=0.127; 7dps-PBS Mean=1.04, SD=0.116; 7dps-PTN Mean=0.954, SD=0.133; 14dps-PBS Mean=0.979, SD=0.0167; 14dps-PTN Mean=1.17, SD=0.289). Kruskal-Wallis test revealed no main effect (P=0.218). B-H) show representative images from each experimental group, detailed in the bottom right corner. MBP is shown in green.

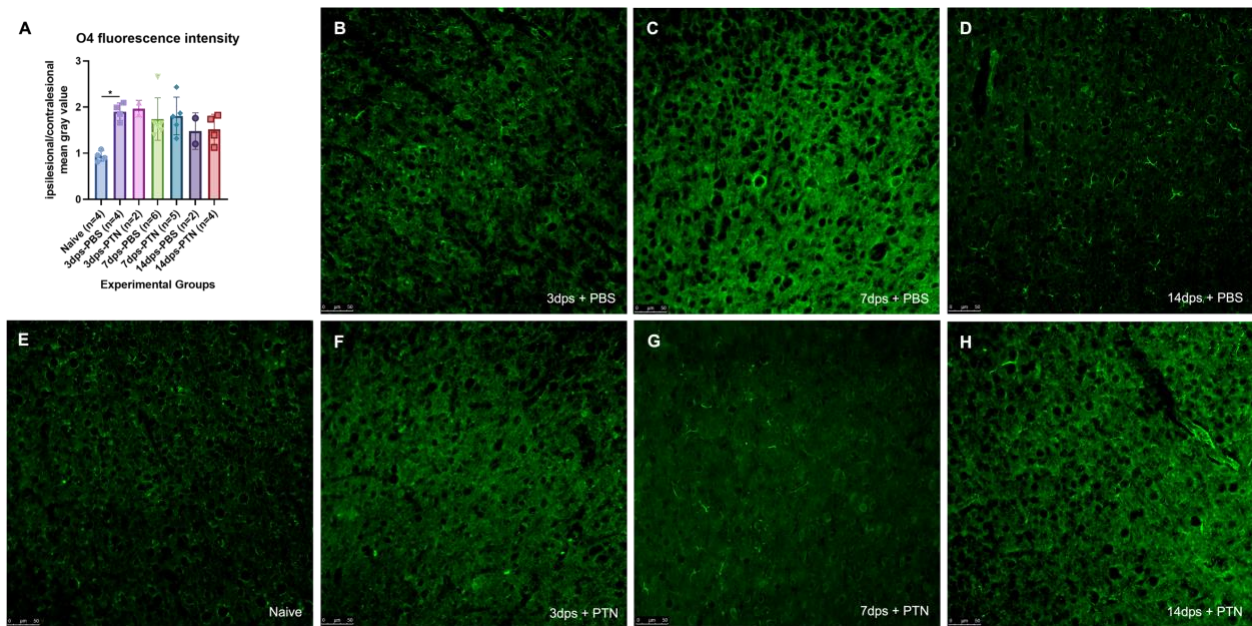


Figure 13. Mean fluorescence intensity of O4 to indicate presence of immature oligodendrocytes from 3 to 14 days post-stroke. The abbreviation “dps” indicates “days post-stroke.” A) Mean fluorescence intensity in each experimental group with error bars showing standard deviation (Naive Mean=0.940, SD=0.114; 3dps-PBS Mean=1.90, SD=0.189; 3dps-PTN Mean=1.97, SD=0.181; 7dps-PBS Mean=1.74, SD=0.460; 7dps-PTN Mean=1.81, SD=0.408; 14dps-PBS Mean=1.48, SD=0.397; 14dps-PTN Mean=1.52, SD=0.324). Kruskal-Wallis test revealed a main effect ($P=0.023$). Dunn’s multiple comparisons test showed a significant difference between Naive and 3dps-PBS groups (marked as * above, $p=0.021$). B-H) show representative images from each experimental group, detailed in the bottom right corner. O4 is shown in green.

Appendix II: Tables

Experimental Group	Male	Male Mean Age (weeks)	Female	Female Mean Age (weeks)	Total	Total Mean Age (weeks)
PBS-STROKE	4	25.93	5	26.29	9	26.13
LPTN-STROKE	5	32.23	4	26.75	9	29.80
HPTN-STROKE	5	26.06	4	26.25	9	26.14
PBS-SHAM	3	30.14	3	25.86	6	28.00
LPTN-SHAM	4	30.75	4	33.89	8	32.32
HPTN-SHAM	4	28.40	5	28.40	9	28.40
NAIVE	5	30.86	5	31.00	10	30.93
TOTAL	30	30.25	30	28.45	60	29.35

Table 1. Information regarding animals that were used in the behavioural assay spanning 8 weeks, from training to endpoint. The above table details the number of each sex in each experimental group, as well as mean age in each experimental group at time of stroke induction.

IHC Series	PTN/DAPI		GFAP/Iba1		MBP/O4	
	Male	Female	Male	Female	Male	Female
Naive	3	2	3	4	3	1
3dps-PBS	2	2	3	1	1	3
3dps-PTN	2	2	3	2	1	1
7dps-PBS	X	X	3	3	3	3
7dps-PTN	X	X	3	2	3	2
14dps-PBS	1	2	1	2	1	1
14dps-PTN	2	2	2	X	1	3

Table 2. Information regarding animals that were used for immunohistochemical analysis. The above table details the number of animals of each sex at each timepoint and treatment group for the investigated markers. Age of animals at stroke induction was 24 to 32 weeks.

	Day 1	Day 2	Day 3	Day 4	Day 5	Day 6	Day 7
Training Week 1	Handling, habituation	Handling, habituation	Train on SP and TB	Train on TB	Train on SP and TB	Rest	Rest
Training Week 2	Train on SP and TB	Train on TB	Baseline Recording for SP and TB	Train on TB	Baseline Recording for SP and TB	Rest	Rest
Stroke & Injections	Stroke Induction	Rest	Cortical Injections	Rest			
1 wps	Assessment on SP and TB	Rest					
2 wps	Assessment on SP and TB	Rest					
3 wps	Assessment on SP and TB	Rest					
4 wps	Assessment on SP and TB	Rest					
5 wps	Assessment on SP and TB	Rest					
6 wps	Assessment on SP and TB	Animals euthanized following last assessment					

Table 3. *Training and testing schedule for animals during the behavioural study.* The abbreviation “wps” indicates “weeks post-stroke.” The column headers indicate the day of the training week, and the row headers indicate the main objectives of each week.

Series	Primary Antibody Target	Marker/What it means
A	Pleiotrophin (PTN)	Pleiotrophin protein
	4'6-diamidino-2-phenylindole (DAPI)	Fluorescent stain that binds to adenine-thymine rich regions of DNA, labelling cell nuclei
B	Glial fibrillary acidic protein (GFAP)	Marker of reactive astrocytes; also used to demarcate the stroke core and measure stroke size
	Ionized calcium-binding adapter molecule (Iba1)	Marker of reactive microglia
C	Myelin basic protein (MBP)	Marker of mature oligodendrocytes and the myelin sheath
	O-antigen (O4)	Marker of pro-oligodendrocytes

Table 4. *Immunohistochemistry (IHC) plan for antibodies and targets.* An outline of how each series of collected tissue will be used to visualize target markers and proteins. The series are collected in such a way that they are each an approximate representation of the brain.

	Controls (n=33)		PBS-Stroke (n=9)		LPTN-Stroke (n=9)		HPTN-Stroke (n=9)	
	Mean	SD	Mean	SD	Mean	SD	Mean	SD
BL1	4.752	2.686	4.566	1.986	5.000	2.317	4.878	4.103
BL2	4.182	2.099	4.844	2.148	5.989	2.187	4.211	3.340
1wps	5.300	2.717	6.333	1.973	6.100	2.102	5.600	3.444
2wps	5.039	2.135	4.622	2.384	4.622	1.154	5.889	3.388
3wps	5.142	2.406	5.400	2.552	5.744	2.021	5.189	2.457
4wps	5.464	1.899	7.189	3.426	5.600	3.035	4.844	1.514
5wps	5.736	2.232	6.378	1.995	5.733	1.780	5.533	2.573
6wps	5.785	2.819	6.222	1.827	5.578	1.092	3.933	2.437

Table 5. *Descriptive statistics of total foot faults during Tapered Beam task.* Mean and standard deviation of total foot faults at each timepoint for each experimental group.

	Controls (n=33)		PBS-Stroke (n=9)		LPTN-Stroke (n=9)		HPTN-Stroke (n=9)	
	Mean	SD	Mean	SD	Mean	SD	Mean	SD
BL	1.000	0.000	1.000	0.000	1.000	0.000	1.000	0.000
1wps	1.313	0.740	1.459	0.491	1.132	0.372	1.388	0.339
2wps	1.317	0.814	1.045	0.401	1.120	0.591	1.578	0.915
3wps	1.363	0.811	1.160	0.226	1.214	0.431	1.374	0.470
4wps	1.589	1.445	1.670	0.941	0.972	0.372	1.426	0.770
5wps	1.570	0.900	1.471	0.849	1.163	0.474	1.559	0.861
6wps	1.615	1.807	1.459	0.569	1.174	0.510	1.012	0.422

Table 6. Descriptive statistics of total foot faults normalized to baseline during Tapered Beam task. Mean and standard deviation of total foot faults normalized to baseline at each timepoint for each experimental group.

	Controls (n=33)		PBS-Stroke (n=9)		LPTN-Stroke (n=9)		HPTN-Stroke (n=9)	
	Mean	SD	Mean	SD	Mean	SD	Mean	SD
BL1	2.494	2.276	2.422	2.504	2.256	1.726	2.256	1.762
BL2	2.445	2.272	2.189	2.620	2.578	2.245	2.144	1.544
1wps	3.218	2.557	3.111	2.904	3.556	1.395	2.767	1.664
2wps	2.745	1.842	1.811	1.489	2.867	2.144	2.667	2.155
3wps	2.858	1.840	2.256	2.968	4.156	1.715	2.500	1.293
4wps	3.121	2.302	3.333	3.777	4.022	2.765	2.467	1.473
5wps	2.788	2.192	2.322	2.572	2.944	2.414	2.611	1.727
6wps	2.845	2.172	2.200	2.519	2.778	2.255	1.522	1.274

Table 7. Descriptive statistics of left foot faults during Tapered Beam task. Mean and standard deviation of left foot faults at each timepoint for each experimental group.

	Controls (n=33)		PBS-Stroke (n=9)		LPTN-Stroke (n=9)		HPTN-Stroke (n=9)	
	<i>Mean</i>	<i>SD</i>	<i>Mean</i>	<i>SD</i>	<i>Mean</i>	<i>SD</i>	<i>Mean</i>	<i>SD</i>
BL	1.000	0.000	1.000	0.000	1.000	0.000	1.000	0.000
1wps	1.888	1.843	1.431	0.879	3.454	4.673	1.297	0.451
2wps	1.677	1.587	0.792	0.250	1.528	1.025	1.082	0.661
3wps	2.149	3.583	0.708	0.524	4.709	7.017	1.327	0.731
4wps	1.803	1.558	1.247	0.778	3.970	6.274	1.175	0.448
5wps	1.584	1.994	0.937	0.437	1.109	0.791	1.350	0.788
6wps	1.920	2.952	0.694	0.464	1.684	1.986	0.662	0.354

Table 8. *Descriptive statistics of left foot faults normalized to baseline during Tapered Beam task.*

Mean and standard deviation of left foot faults normalized to baseline at each timepoint for each experimental group.

	Naive (n=10)		Stroke (n=8)	
	<i>Mean</i>	<i>SD</i>	<i>Mean</i>	<i>SD</i>
BL 1	5.070	3.283	4.350	2.672
BL 2	4.010	2.324	4.150	2.437
1wps	4.740	2.367	6.038	2.270
2wps	5.580	1.954	4.575	2.861
3wps	4.550	2.055	4.400	1.552
4wps	5.300	1.614	5.538	3.258
5wps	5.540	2.261	5.713	2.105
6wps	4.190	1.734	5.513	2.377

Table 9. *Descriptive statistics of total foot faults during Tapered Beam task for selected animals.*

Mean and standard deviation of total foot faults at each timepoint for each experimental group.

	Naive (n=10)		Stroke (n=8)	
	Mean	SD	Mean	SD
BL	1.000	0.000	1.000	0.000
1wps	1.100	0.297	1.615	0.545
2wps	1.432	0.674	1.137	0.457
3wps	1.121	0.473	1.219	0.495
4wps	1.367	0.606	1.649	1.245
5wps	1.449	0.808	1.633	0.740
6wps	1.036	0.395	1.428	0.464

Table 10. Descriptive statistics of total foot faults normalized to baseline during Tapered Beam task for selected animals. Mean and standard deviation of total foot faults normalized to baseline at each timepoint for each experimental group.

	Naive (n=10)		Stroke (n=8)	
	Mean	SD	Mean	SD
BL 1	1.970	1.283	1.163	1.124
BL 2	1.880	1.783	1.738	2.181
1wps	2.020	1.420	3.000	2.327
2wps	2.770	1.911	1.575	1.516
3wps	2.070	1.228	2.463	1.865
4wps	2.540	1.839	3.150	2.568
5wps	2.430	1.960	1.738	2.208
6wps	1.730	1.561	1.863	2.411

Table 11. Descriptive statistics of left foot faults during Tapered Beam task for selected animals. Mean and standard deviation of left foot faults at each timepoint for each experimental group.

	Naive (n=10)		Stroke (n=8)	
	Mean	SD	Mean	SD
BL	1.000	0.000	1.000	0.000
1wps	1.271	0.749	3.728	4.935
2wps	1.554	0.815	1.130	0.822
3wps	1.248	0.552	4.829	7.536
4wps	1.459	0.934	4.382	6.602
5wps	1.547	1.357	1.000	0.669
6wps	0.980	0.768	1.572	2.128

Table 12. Descriptive statistics of left foot faults normalized to baseline during Tapered Beam Task for selected animals. Mean and standard deviation of left foot faults normalized to baseline at each timepoint for each experimental group.